AD-774 801

MATERIAL PROPERTIES FOR POSTSHOT MIXED COMPANY ANALYSIS: RECOMMENDATIONS BASED ON RECENT LABORATORY AND IN SITU TEST DATA

John Q. Ehrgott, et al

Army Engineer Waterways Experiment Station

Prepared for:

Defense Nuclear Agency

January 1974

DISTRIBUTED BY:

NTIS

National Technical Information Service
U. S. DEPARTMENT OF COMMERCE
5285 Port Royal Road, Springfield Va. 22151

Unclassified

SECURITY CLASSIFICATION OF THIS PAGE (When Data Entered)

AD-774801

REPORT DOCUMENTATION PAGE	READ INSTRUCTIONS BEFORE COMPLETING FORM
1. REPORT NUMBER: Miscellaneous Paper S-74-1	2. GOVT ACCESSION NO. / 3. RECIPIENT'S CATALOG NUMBER
4. TITLE (and Subtitle): MATERIAL PROPERTIES FOR POSTSHOT MIXED COMPANY ANALYSIS: RECOMMENDATIONS BASED ON RECENT LABORATORY AND IN SITU TEST DATA	5. TYPE OF REPORT & PERIOD COVERED: Final report
	6. PERFORMING ORG. REPORT NUMBER
7. AUTHOR(s): John Q. Ehrgott, John G. Jackson, Jr.	8. CONTRACT OR GRANT NUMBER(s)
9. PERFORMING ORGANIZATION NAME AND ADDRESS: U. S. Army Engineer Waterways Experiment Station, Soils and Pavements Laboratory, P. O. Box 631, Vicksburg, Miss. 39180	10. PROGRAM ELEMENT, PROJECT, TASK AREA & WORK UNIT NUMBERS: Subtask SB209, Work Unit 11
11. CONTROLLING OFFICE NAME AND ADDRESS: Defense Nuclear Agency, Washington, D. C. 20305	12. REPORT DATE: January 1974
	13. NUMBER OF PAGES: ~~89~~ 80
14. MONITORING AGENCY NAME & ADDRESS (if different from Controlling Office)	15. SECURITY CLASS. (of this report): Unclassified
	15a. DECLASSIFICATION/DOWNGRADING SCHEDULE

16. DISTRIBUTION STATEMENT (of this Report)

Approved for public release; distribution unlimited.

17. DISTRIBUTION STATEMENT (of the abstract entered in Block 20, if different from Report)

Reproduced by
NATIONAL TECHNICAL
INFORMATION SERVICE
U S Department of Commerce
Springfield VA 22151

18. SUPPLEMENTARY NOTES

This research was sponsored by the Defense Nuclear Agency under Subtask SB209, Work Unit 11, "Laboratory Studies of the Response of Soil and Rock to Blast-Type Loadings."

19. KEY WORDS (Continue on reverse side if necessary and identify by block number)

Field tests
Geologic materials
Ground motion
Laboratory tests
Mixed Company (Event III)
Rock properties
Soil properties

20. ABSTRACT (Continue on reverse side if necessary and identify by block number)

An idealized, horizontally layered geologic profile and an associated set of constitutive properties for each layer in this profile were developed during FY 1972 for use in pretest ground motion calculations for Mixed Company Event III, a 500-ton high explosive test. The study reported herein was conducted during FY 1973 to evaluate the validity of the preshot recommendations in the light of new data and to make appropriate recommendations for a revised site profile and a revised set of constitutive properties for use in a

DD FORM 1 JAN 73 1473 EDITION OF 1 NOV 65 IS OBSOLETE

Unclassified

SECURITY CLASSIFICATION OF THIS PAGE (When Data Entered)

ABSTRACT (Continued)

postshot recalculation of the event. The pretest calculational grid extended only to a depth of about 300 feet. Examination of possible travel paths showed that reflection from deeper interfaces could have arrived in time to influence the ground motions measured during Event III. Therefore, it was recommended that the recalculation grid extend to depths of 500 to 600 feet, i.e., into the Precambrian basement. Tests on samples taken just after the event showed that water content changes due to the wet weather conditions at shot time substantially affected the compressibility of the upper 2 to 3 feet of overburden soil. Thus, it was recommended that the overburden soil be idealized into two layers rather than into one as originally recommended for preshot calculations. An extensive reanalysis of the available surface refraction survey data, along with analysis of the Event III ground motion data, resulted in revisions to the entire seismic velocity profile and, hence, to the associated values of the initial uniaxial strain modulus. The stress levels associated with these moduli were originally assumed to be quite low, e.g., less than 10 psi for the Kayenta Formation materials. A lower bound value of 50 psi was recommended as being more reasonable for the initial Kayenta "precursor" stress. This phenomenon appears to be a function of loading rate. Tests on the Kayenta materials also revealed that horizontal-to-vertical anisotropy undoubtedly affected the ground motion results, but the problem of how to utilize the various horizontal and vertical data to specify meaningful "effective" or "average" isotropic property values still remains. As a result of recent test data from Lawrence Livermore Laboratory, however, substantial changes have been made in the recommended failure envelopes, which now reflect a highly nonlinear behavior, including significant strength increases at high pressure.

THE CONTENTS OF THIS REPORT ARE NOT TO BE USED FOR ADVERTISING, PUBLICATION, OR PROMOTIONAL PURPOSES. CITATION OF TRADE NAMES DOES NOT CONSTITUTE AN OFFICIAL ENDORSEMENT OR APPROVAL OF THE USE OF SUCH COMMERCIAL PRODUCTS.

PREFACE

This paper was prepared for presentation at the Defense Nuclear Agency (DNA) Strategic Structures Long-Range Planning Meeting (LRPM) held at the Stanford Research Institute, Menlo Park, California, during 15 to 17 May 1973. The work described herein was conducted by the U. S. Army Engineer Waterways Experiment Station (WES) for DNA under Subtask SB209, Work Unit 11, "Laboratory Studies of the Response of Soil and Rock to Blast-Type Loadings." Mr. C. B. McFarland was the DNA Project Officer for Subtask SB209.

The study was performed by personnel of the WES Soils and Pavements Laboratory (S&PL). Mr. R. W. Peterson, Soil Dynamics Division (SDD), S&PL, conducted the laboratory tests. The analyses were performed by Mr. J. Q. Ehrgott, who presented the results at the LRPM. Mr. J. R. Curro, Jr., Earthquake Engineering and Vibrations Division, S&PL, provided helpful comments and interpretations regarding the seismic refraction survey data, and Dr. P. F. Hadala, SDD, S&PL, provided valuable advice and guidance throughout the study. The paper was jointly prepared by Mr. Ehrgott and Dr. J. G. Jackson, Jr., Chief, SDD.

BG E. D. Peixotto, CE, and COL G. H. Hilt, CE, were Directors of WES and Mr. F. R. Brown was Technical Director during the conduct of this study and the preparation of this paper. Mr. J. P. Sale and Mr. R. G. Ahlvin were Chief and Assistant Chief, S&PL, respectively.

CONTENTS

FIGURES

FIGURES

FIGURES

CONVERSION FACTORS, BRITISH TO METRIC UNITS OF MEASUREMENT

British units of measurement used in this report can be converted to metric units as follows:

Multiply	By	To Obtain
feet	0.3048	meters
tons	907.1846	kilograms
feet per second	0.3048	meters per second
pounds (mass) per cubic foot	16.0185	kilograms per cubic meter
pounds (force) per square inch	0.6894757	newtons per square centimeter
kips (force) per square inch	0.6894757	kilonewtons per square centimeter
pounds (force) per square inch per second	0.6894757	newtons per square centimeter per second

CHAPTER 1

INTRODUCTION

1.1 BACKGROUND

A geologic profile for the Mixed Company site and associated constitutive properties for each layer in this profile were developed during FY 1972 by the U. S. Army Engineer Waterways Experiment Station (WES). The idealized profile and properties (Reference 1) were disseminated in June 1972 for use in developing fits to constitutive models that were in turn used for pretest ground motion calculations (Reference 2) of Event III, a 500-ton[1] high explosive test. Since these properties were disseminated, additional field and laboratory test data, as well as ground shock data from the event itself and from the Air Force Weapons Laboratory's (AFWL) Cylindrical In Situ Test (CIST) explosive experiment, have become available.

Ground shock data obtained both by WES and AFWL were presented at the Mixed Company project review meeting in March 1973. The pretest ground motion predictions did not agree very well with either set of measurements. The calculated arrival times for the initial ground motions were much later than those indicated by the field measurements, and the general characteristics of the calculated wave forms did not match those of the field data. A number of assumptions were made in the process of developing the preshot profile and property idealizations (Reference 3), which if not valid could well account for the observed discrepancies between the field measurements and the calculated ground motions. It should also be noted that the mathematical models had to be hurriedly fit in order to meet the schedule for the pretest calculation, and they did not closely replicate all facets of the recommended constitutive properties. Also, the calculational grid did not extend deep

---

[1] A table of factors for converting British units of measurement to metric units is presented on page 9.

enough to incorporate the reflecting interface between the Triassic sedimentary materials and the Precambrian basement rock. Thus, there are sufficient uncertainties to warrant: (1) a reevaluation of the profile and properties in the light of the newly available data, and (2) a recalculation of Event III with a much more precise fit to the constitutive properties and profile resulting from this reevaluation.

1.2 PURPOSES

The purposes of this study were to evaluate the validity of the preshot Mixed Company Event III site profile and the associated set of constitutive properties in light of new data and to make appropriate recommendations for a revised site profile and a revised set of constitutive properties for use in a postshot recalculation of the event.

1.3 SCOPE

This paper presents the results of a reevaluation of the Mixed Company site profile and constitutive properties utilizing both field and laboratory data. Revisions to the subsurface profile were based primarily on the water contents determined in the soil overburden at shot time. An extensive reanalysis of the seismic velocity data was conducted. New constitutive property recommendations for the overburden soil were developed based on laboratory tests conducted on specimens taken in the field just a few days after the event. The properties of the Kayenta Formation were revised to consider the effect of loading rate on the initial portion of the uniaxial strain (UX) test stress-strain curves, the effects of anisotropy on the observed triaxial shear (TX) and UX test behaviors, and the correlation observed between shear strength obtained from laboratory tests and strength obtained from an in situ test.

CHAPTER 2

SITE PROFILE

In developing the pretest calculation profile for the Mixed Company Event III site, many assumptions were necessary in order to translate the available data into an idealized, horizontally layered profile. The purpose of this chapter is to evaluate these assumptions in the light of additional information and analyses and to recommend appropriate revisions. As was the case for the original profile, the revised profile is intended to be an idealized representation of conditions along the WES gage line.[1]

2.1 DEPTHS TO MAJOR GEOLOGIC INTERFACES

Four major geologic interfaces were originally defined for the site profile. The first, at a depth of 5 feet, depicted the change from soil overburden to the complex Kayenta Formation of intermixed siltstones, sandstones, mudstones, and conglomerates. At 70 feet, the sandstones of the Wingate Formation were assumed to be encountered, followed by Chinle Formation siltstone at 400 feet. Finally, an interface with the Precambrian basement complex was set at a depth of 500 feet. No reason has been found to alter these interface depths. The pretest calculational grid, however, extended only to a depth of approximately 300 feet and thus included only the overburden soil, the Kayenta Formation, and a portion of the Wingate. Since that time, several calculations have been made for other projects that indicate that near-surface ground motions can be significantly affected by reflections from very deep geologic interfaces. This determination prompted an examination of the profile to see if signals from the omitted Mixed Company interfaces were being

---

[1] Two gage lines were installed for Event III, one by WES and one by AFWL. A rolled fill was constructed along the WES line in an attempt to provide a uniform 5-foot-thick layer of soil overburden; fill was not placed along the AFWL line, and the natural soil cover varied in thickness from 3-1/2 to 5 feet.

recorded. Figure 1 shows the subsurface profile to a range of 1,400 feet and to a depth of 500 feet. Also shown are travel paths that are possible for some of the reflected waves and the surface arrival times of these waves based on an assumed 7,500 ft/sec wave speed in both the Kayenta and Wingate Formations. This approximate model shows that signals reflected from the Chinle and Precambrian layers could have arrived in time to influence the ground motions measured during Event III, since significant near-surface motion occurred for at least 500 msec at most of the ranges shown in the figure. It is therefore strongly recommended that the grid used in any Mixed Company recalculation extend into the Precambrian basement complex.

2.2 IDEALIZATION OF PRIMARY GEOLOGIC UNITS

As denoted above, the site profile encompasses five primary geologic units, i.e., the soil overburden, Kayenta sandstones, Wingate sandstones, Chinle siltstones, and the Precambrian basement rocks. In the idealized pretest profile, the overburden soil was represented as a single horizontal layer, Layer I. The underlying Kayenta Formation, however, was subdivided into four layers: Layer II, representing the weathered siltstone; Layer III, the upper one-fourth of the unweathered Kayenta rock; Layer IV, an artificial layer representing the softer Kayenta material occurring randomly throughout the formation; and Layer V, the lower three-fourths of the unweathered Kayenta rock. The Wingate, Chinle, and Precambrian Formations were each represented by one layer, Layers VI, VII, and VIII, respectively. In making this idealization, it was assumed that the water content and density of the constructed berm would match those of the natural soil overburden and also that the water content and other compositional properties found to exist at the time samples were extracted from the site would be the same as those existing at the time of actual detonation.

Wet weather conditions existed at the site just prior to Event III, and the water content of the upper 2 to 3 feet of overburden soil increased from an average of about 7 percent, as determined at the time preshot properties were developed, to about 15 percent at the time of

the shot. The variations in water content and dry density with depth in the top 5 feet in a section in natural soil are shown in Figure 2. From the surface to a depth of approximately 2 feet, the water content at shot time appears to have been approximately 15 to 16 percent; at depths below 3 feet, however, the available data indicate that the water content may not have changed significantly from the original value of about 7 percent. The variation in dry density with depth shown in Figure 2 indicates that no significant change in that composition property had occurred since the time of the pretest investigation. Figure 3 shows the dry density and water content profile for a composite section of fill and natural soil. The water content profile is essentially the same as that shown in Figure 2; the dry density profile, however, is quite different. The density of the fill itself appears to be very uniform, but the upper 1/2 to 1 foot of natural soil underlying the fill apparently increased in density due to compaction that occurred during construction of the berm.

Primarily on the basis of the data shown in Figures 2 and 3, it is recommended that the soil overburden along the main WES gage line be idealized into two horizontal layers for postshot calculations rather than into one as originally recommended for preshot calculations.

The postshot water content and densities of the Kayenta materials did not differ from the pretest values sufficiently to warrant a revision in the subdivision of the Kayenta Formation. Although the wet density of the upper one-fourth of the unweathered Kayenta material was lower by approximately 2 pcf than the pretest density, it was assumed that the new value simply represented a better definition of the density for that material rather than an alteration due to the blast or change in climate. None of the clayey conglomerate material, which was arbitrarily placed at the 18- to 22-foot depth to form Layer IV in the pretest idealized profile, was encountered in any of the four 20-ft-deep posttest borings. Therefore, the composition properties for this material could not be reevaluated.

No additional new data were obtained in order to evaluate the preshot idealizations recommended for the deep formations underlying the

Kayenta. However, the geologic information, the limited dry density data obtained on field samples taken at outcrops, and the water content values that were previously assumed were reviewed. As a result, it was again decided that the Wingate, Chinle, and Precambrian Formations should not be subdivided but that each can be adequately depicted as a single idealized horizontal layer for calculational purposes.

2.3 RECOMMENDED POSTSHOT PROFILE

The recommended postshot profile and composition properties are summarized in Table 1, which lists the numbers of the old preshot layers and those of the new postshot layers, the material description, the depth range for each layer, and the values of wet density, water content, and the volume of air now judged to most nearly represent conditions along the WES gage line. There are two significant differences between this profile and the pretest profile. First, the soil overburden has been subdivided into two layers, Layers 1A and 1B. However, if the calculational grid cannot be zoned fine enough to effect this recommended subdivision, then a composite layer, Layer 1C, has also been defined to represent the total zone of fill and natural soil overburden.

Second, it is recommended that the artificial Layer IV, formerly located between a depth of 18 and 22 feet, be eliminated from the postshot calculation profile, at least initially. With the uncertainties surrounding the definition of seismic velocities and constitutive properties, as will be discussed later, it appears that the most practical approach would be to keep the profile as simple as possible for the planned recalculation. However, the basic assumption of lumping small zones of material, which cannot be incorporated in the profile due to computational grid-size limitations, into one or more large layers should be evaluated in future parametric studies.

TABLE 1 RECOMMENDED POSTSHOT PROFILE AND COMPOSITION PROPERTIES

Layer Number		Material Description	Depth, ft		Wet Density pcf	Water Content pct	Volume of Air pct
Preshot	Postshot		From	To			
I	1A	Fill and/or top portion of overburden soil	0	2-1/2	120.1	15.5	11.7
	1B	Bottom portion of overburden soil	2-1/2	5	111.3	7.0	25.9
	1C	Composite of fill and natural soil	0	5	116.5	12.0	17.5
II	2	Weathered Kayenta material	5	9	137.0	3.5	12.8
III	3	Upper 1/4 unweathered Kayenta material	9	24	145.0	4.5	6.4
V	4	Lower 3/4 unweathered Kayenta material	24	70	147.0	4.5	5.1
VI	5	Wingate sandstone	70	400	128.4	7.0	14.0
VII	6	Chinle siltstone	400	500	158.0	--	--
VIII	7	Precambrian basement rock	>500		162.0	--	--

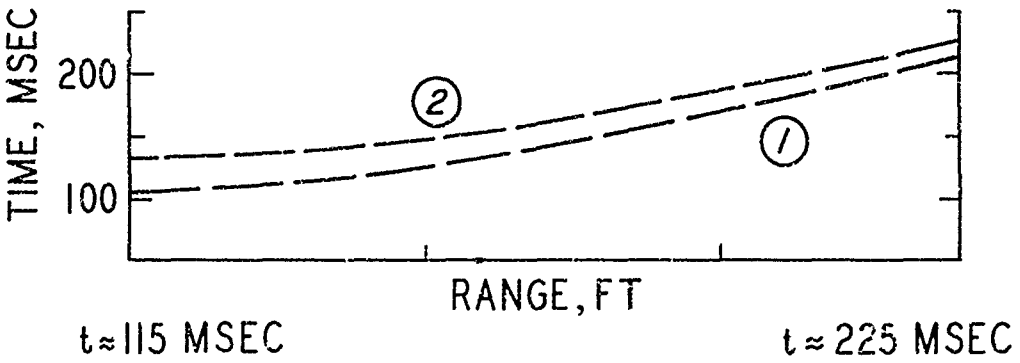

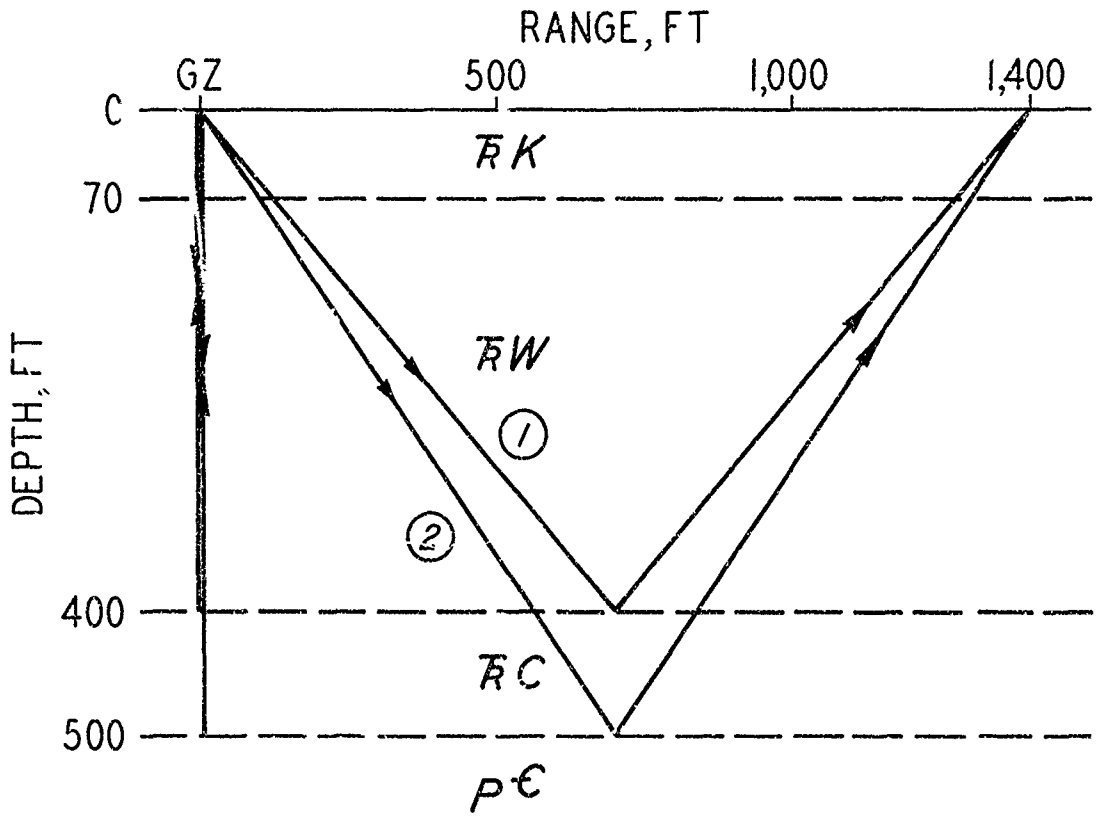

Figure 1 Subsurface profile showing possible paths of waves reflected from deep geologic interfaces and corresponding arrival times at the ground surface.

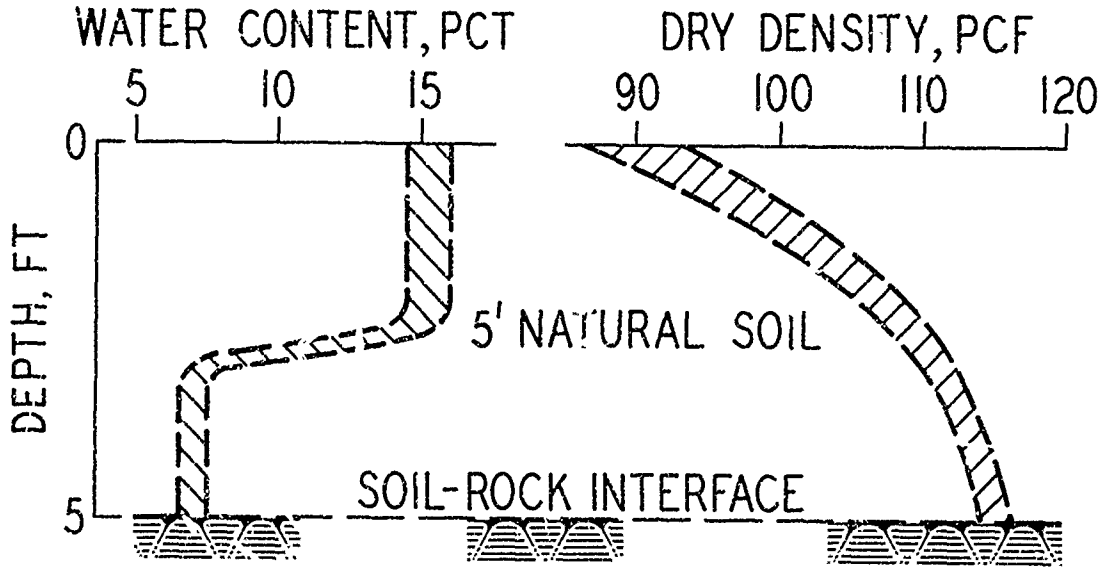

Figure 2 Profile of natural soil overburden layer showing variation of water content and dry density with depth.

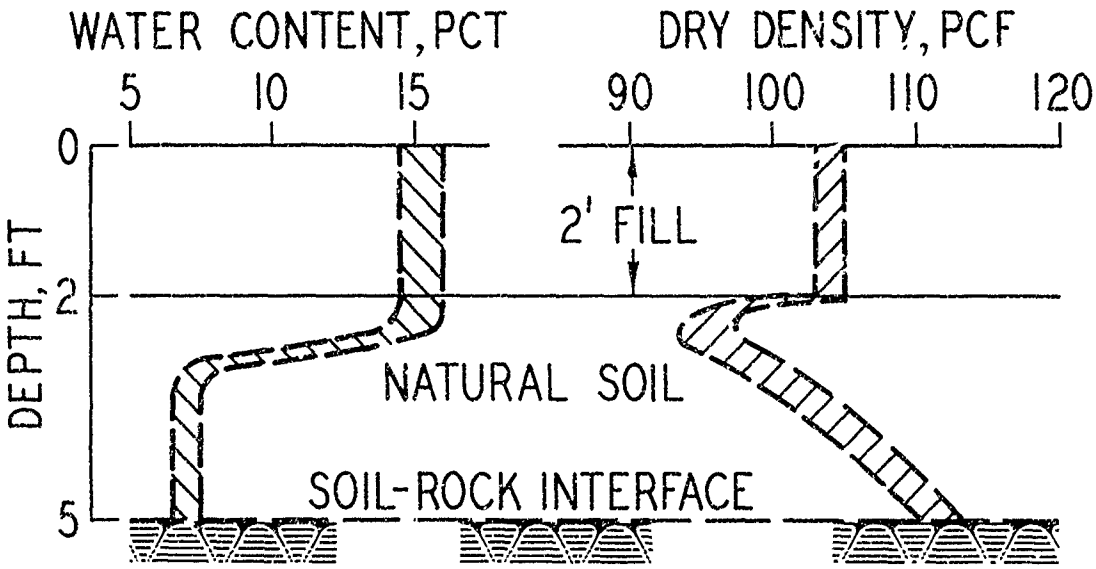

Figure 3 Profile of composite fill and natural soil overburden layer showing variation of water content and dry density with depth.

CHAPTER 3

SEISMIC VELOCITIES

If the seismic velocities used with the calculation profile do not match those of the real site profile, then calculated arrival times obviously cannot agree with field-measured data. Neither can the calculated wave forms match the field wave forms, since the calculated wave arrivals will be incorrectly phased. For this reason, an important key to an adequate calculation of Mixed Company Event III is the correct definition of seismic velocities. The analyses originally applied to the seismic velocity data from 22 surface refraction lines are documented in the summary report (Reference 1); however, these data, along with those available from four other refraction lines surveyed near the test site, have now been reexamined with respect to the overall topography of the area. In addition, data from the AFWL CIST experiment have provided new information on horizontal wave velocities, and the arrival-time data from Event III itself have been analyzed as a refraction survey to deduce possible seismic velocity profiles. The purpose of this chapter is to present the results of these various examinations and to recommend seismic velocity values for the site profile developed in Chapter 2 for postshot calculations.

3.1 REANALYSIS OF SURFACE REFRACTION SURVEY DATA

A plan view of the Mixed Company site showing seismic survey locations with respect to the Event III ground zero (GZ), the WES and AFWL gage lines, and the AFWL CIST experiment is shown in Figure 4. Seismic velocity data from 21 hammer-source surface refraction lines, each 150 feet long with 15-foot geophone spacings, and one 570-foot-long explosive line were obtained from the immediate vicinity of GZ (Reference 4). The short-line (150-foot-long) data indicated velocities ranging from 2,100 to 3,200 ft/sec in the upper 9 feet (i.e., a combination of soil overburden and weathered Kayenta siltstone) and velocities ranging from 6,000 to 8,800 ft/sec in the immediately underlying unweathered Kayenta rock. In the pretest analysis, a value of 1,800 ft/sec was

estimated for the overburden soil, a value of 2,500 ft/sec for the weathered Kayenta, and values of 7,100 ft/sec for the upper one-fourth of the unweathered Kayenta and 7,500 ft/sec for the lower three-fourths.

The long-line (570-foot-long) survey indicated a zone of 14,000-ft/sec material at a depth of about 100 feet, but this value was not recommended for preshot calculations since it was believed to be too high to be representative of the low-density Wingate sandstone expected at that depth; a pretest value of 7,400 ft/sec was recommended. None of the refraction lines were long enough to provide seismic velocities for the Chinle siltstone and the Precambrian basement; values of 9,000 and 15,000 ft/sec, respectively, were estimated for these final two layers of the pretest profile.

Seismic surveys, each consisting of 25-, 50-, and 600-foot-long refractions lines, were also run at the four locations shown in Figure 4 that lie between the main WES gage line and the northwest-trending mesa. The data from these surveys were not considered in the initial analysis; however, they were subsequently examined since the short lines were run with 5-foot geophone spacings that enabled the seismic velocities in the overburden soil (ranging from 1,000 to 1,400 ft/sec with an average of 1,100 ft/sec) to be distinguished from those in the weathered siltstone (ranging from 1,800 to 5,000 ft/sec with an average of 3,300 ft/sec).

Velocities in the deeper, more competent Kayenta material seemed to be related to the areal topography. Four cross sections through the site are depicted in Figure 5. The geologic formation interfaces were estimated from visual observations of the various mesa and canyon walls; the Kayenta-Wingate interface appeared to roughly follow the surface slope. The available seismic survey data have been projected onto two of the cross sections (Sections C-C and D-D); the lower velocity zones (4,000 to 6,000 ft/sec) of the upper Kayenta material appeared to be confined to the lower elevation drainage patterns, while higher velocities (7,000 to 8,000 ft/sec) indicative of a more resistant material were recorded in the higher elevation area around GZ. Velocities for the lower Kayenta materials in either case appeared to be on the order of 8,000 to 10,000 ft/sec. As shown in Figure 4, the WES gage lines

are located entirely along a knoll where 7,000- to 8,000-ft/sec velocities should typify the upper unweathered Kayenta material. Along the AFWL gage line, however, two profiles may exist. Close to GZ (<300 feet), the profile should be similar to that under the WES gage line, but farther out as the terrain drops off the upper Kayenta velocities may be on the order of 4,000 to 6,000 ft/sec.

Although the four early 600-foot line surveys easily penetrated the Wingate formation, none detected a velocity increase over the lower Kayenta. The Wingate could have had a lower seismic velocity than the Kayenta, but this difference could only have been detected with an uphole rather than a refraction-type field survey. Seismic velocity measurements made in the laboratory on samples of Wingate sandstone were in fact lower than similar measurements made on the overlying Kayenta samples. The four lines were too short, however, to penetrate the Chinle and Precambrian Formations; however, laboratory tests have indicated that seismic velocities of approximately 11,000 and 18,000 ft/sec, respectively, should be expected.

3.2 ANALYSIS OF EXPLOSIVE TEST DATA

On 28 September 1972, AFWL conducted a 35-foot-deep CIST experiment about 1 mile to the southeast of the Mixed Company Event III GZ (see Figure 4.). The first arrival-time data indicated horizontal seismic velocities in the upper unweathered Kayenta material ranging from about 10,000 ft/sec to about 20,000 ft/sec (Reference 5). These velocities were much higher than those indicated by the surface refraction surveys. Since they were measured along a horizontal plane, they may indicate a significant horizontal-to-vertical anisotropy for the Kayenta material. Even so, 20,000-ft/sec velocities are generally associated with sound igneous rocks, such as granite, rather than with relatively soft sedimentary rocks such as siltstone and sandstone. A cross-hole seismic survey at the Mixed Company site is definitely recommended to assist in resolving this uncertainty. Since the CIST measurements were obtained at higher elevations than any of the other measurements, it may also be

possible that the velocity differences are due to material and/or geologic differences.

Event III was detonated on 13 November 1972. Shock-front diagrams were constructed by both WES (Reference 6) and AFWL (Reference 7) based on the arrival times recorded by their respective motion gages. These diagrams indicated that the soil overburden had an average seismic velocity of about 1,300 ft/sec; this agrees quite well with the 1,100-ft/sec velocity value determined by the refraction surveys. The data indicate velocities on the order of 3,500 ft/sec for the weathered siltstone stratum; again, this is in excellent agreement with the 3,300-ft/sec average determined from the refraction data. The data also indicate velocities for the unweathered Kayenta materials in the 8,000- to 10,000-ft/sec range, which are also consistent with the refraction survey results.

The only gages placed deep enough to be in the Wingate sandstone were those directly under GZ. It is possible that, in this region where the travel paths essentially paralleled the gage columns, the grout used to fill the gage columns may have influenced the arrival times, since it had a higher P-wave velocity (i.e., about 10,000 ft/sec) than the overall mass of natural materials. However, the shock-front diagram data are insufficient to permit a definite conclusion in this regard.

The near-surface (1-1/2-foot-deep) motion gage results, however, can be analyzed as a long-line, surface refraction survey to extract some seismic velocity information for the Wingate and deeper formations.[1] One such analysis of the data obtained along the WES gage lines (LN302 and LN311W) was reported by Ballard and Leach (Reference 8). It indicated a single 570-foot-thick stratum of 8,300-ft/sec material overlying 18,000-ft/sec material (see Example A in Figure 6). Other interpretations or fits to the data are possible, as indicated by

---

[1] This technique will not provide valid information for the materials above a depth of about 60 to 70 feet since the airblast-dominated range of superseismic motion is the "effective" geophone spacing for the survey.

Examples B, C, and D in the insert in Figure 6. When the layer velocities do not monotonically increase with depth, as is the case with Examples B and C, the layer interface depths cannot be calculated from the refraction equations; therefore, only a rough estimate is possible.

3.3 RECOMMENDED POSTSHOT SEISMIC VELOCITIES

The shock-front or arrival-time diagrams from Event III and the recently analyzed short-line refraction surveys both indicate that the 1,800-ft/sec seismic velocity originally recommended for the soil overburden was too high; a value of 1,300 ft/sec is now recommended for postshot calculation models. Conversely, the arrival-time data and the short-line refraction data indicated that the 2,500-ft/sec velocity previously recommended for the immediately underlying weathered siltstone was too low; a value of 3,500 ft/sec is now recommended.

Reanalysis of all of the available surface refraction data indicates that velocities in the unweathered Kayenta materials depend on the areal topography, with values within the ranges shown in Figure 7. Along the WES gage line, a specific value of 8,000 ft/sec is now recommended for the upper one-fourth of the unweathered Kayenta, and 10,000 ft/sec is recommended for the lower three-fourths. Previously recommended values were 7,100 and 7,500 ft/sec, respectively.

As shown in Figure 7, a variety of field values were obtained for depths associated with the Wingate sandstone, but all exceeded 8,000 ft/sec; laboratory tests, however, gave values consistently lower than 8,000 ft/sec. A velocity of 8,000 ft/sec is now recommended in lieu of the previous value of 7,400 ft/sec. Based solely on laboratory test data, Chinle siltstone velocities are now believed to be on the order of 11,000 rather than 9,000 ft/sec as originally recommended. Finally, the Precambrian basement velocity is now believed to be at least 18,000 ft/sec rather than 15,000 ft/sec. This conclusion was derived from both the Event III arrival-time analysis and the recent laboratory test results.

These current best estimates of the seismic velocities associated with each of the layers in the idealized geologic profile beneath the

WES gage line are summarized in Table 2. Previously recommended values are also tabulated for comparison.

TABLE 2 RECOMMENDED SEISMIC VELOCITY VALUES

Layer Number	Material Description	Depth, ft		Seismic Velocity, ft/sec	
		From	To	Original	Recommended
1A	Fill and/or top portion of overburden soil	0	2-1/2	1,800	1,300
1B	Bottom portion of overburden soil	2-1/2	5	1,800	1,300
1C	Composite of fill and natural soil	0	5	1,800	1,300
2	Weathered Kayenta material	5	9	2,500	3,500
3	Upper 1/4 unweathered Kayenta material	9	24	7,100	8,000
4	Lower 3/4 unweathered Kayenta material	24	70	7,500	10,000
5	Wingate sandstone	70	400	7,400	8,000
6	Chinle siltstone	400	500	9,000	11,000
7	Precambrian basement rock	>500		15,000	18,000

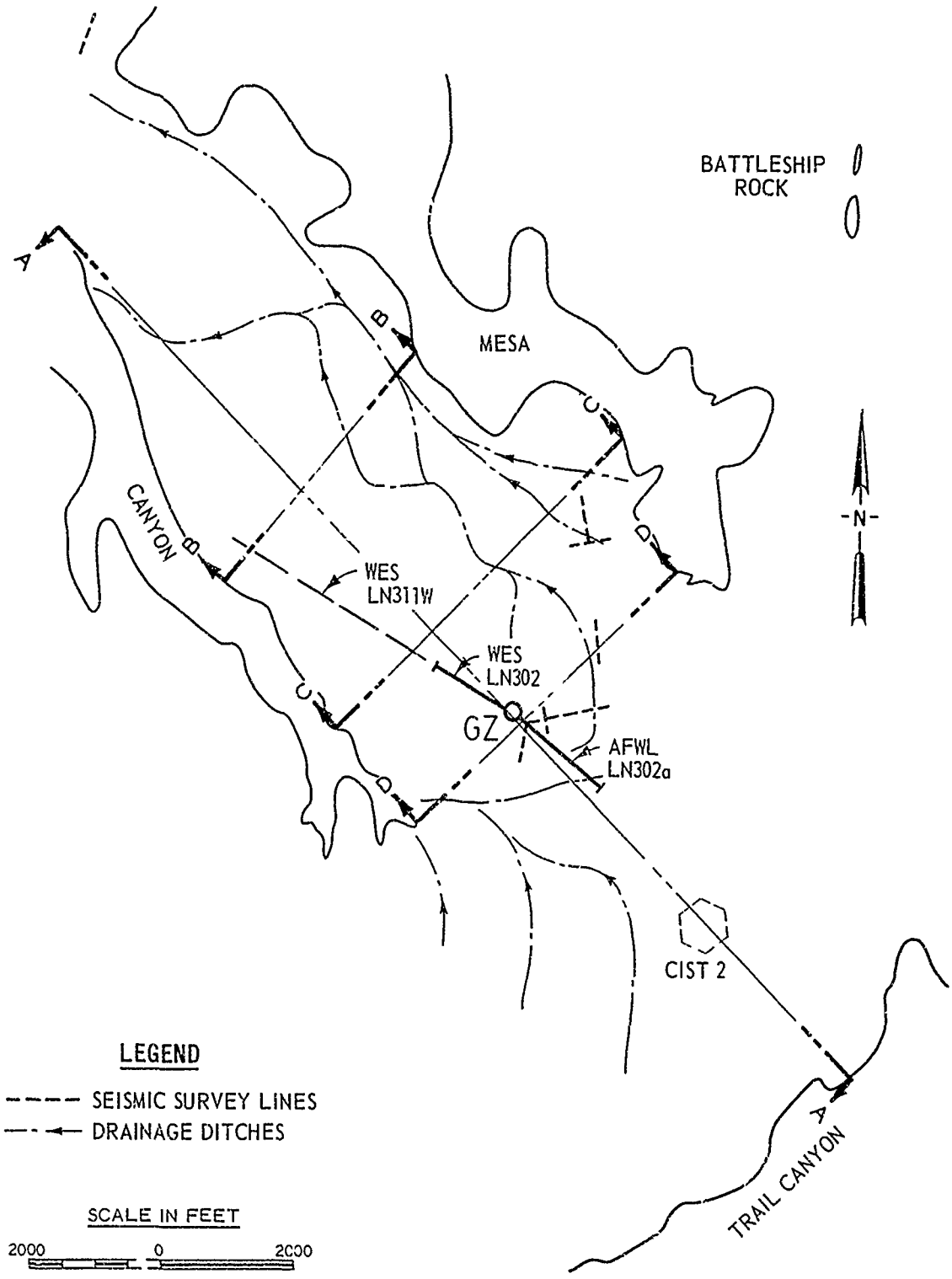

Figure 4 Plan view of Mixed Company site showing seismic survey locations with respect to the Event III GZ, the WES and AFWL gage lines, and the AFWL CIST experiment.

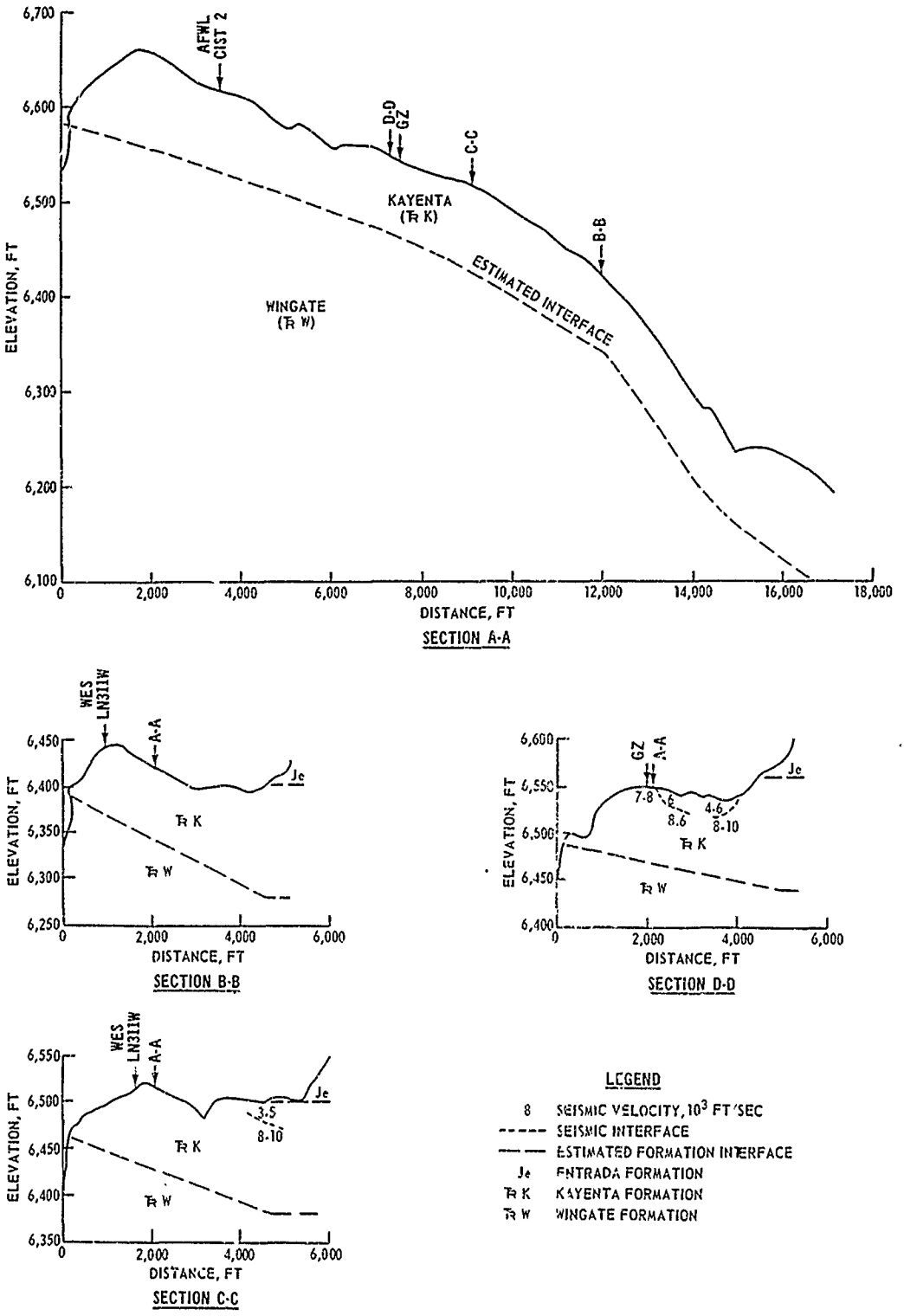

Figure 5 Cross sections through Mixed Company site (see Figure 4) indicating seismic velocities and estimated seismic and geologic interfaces.

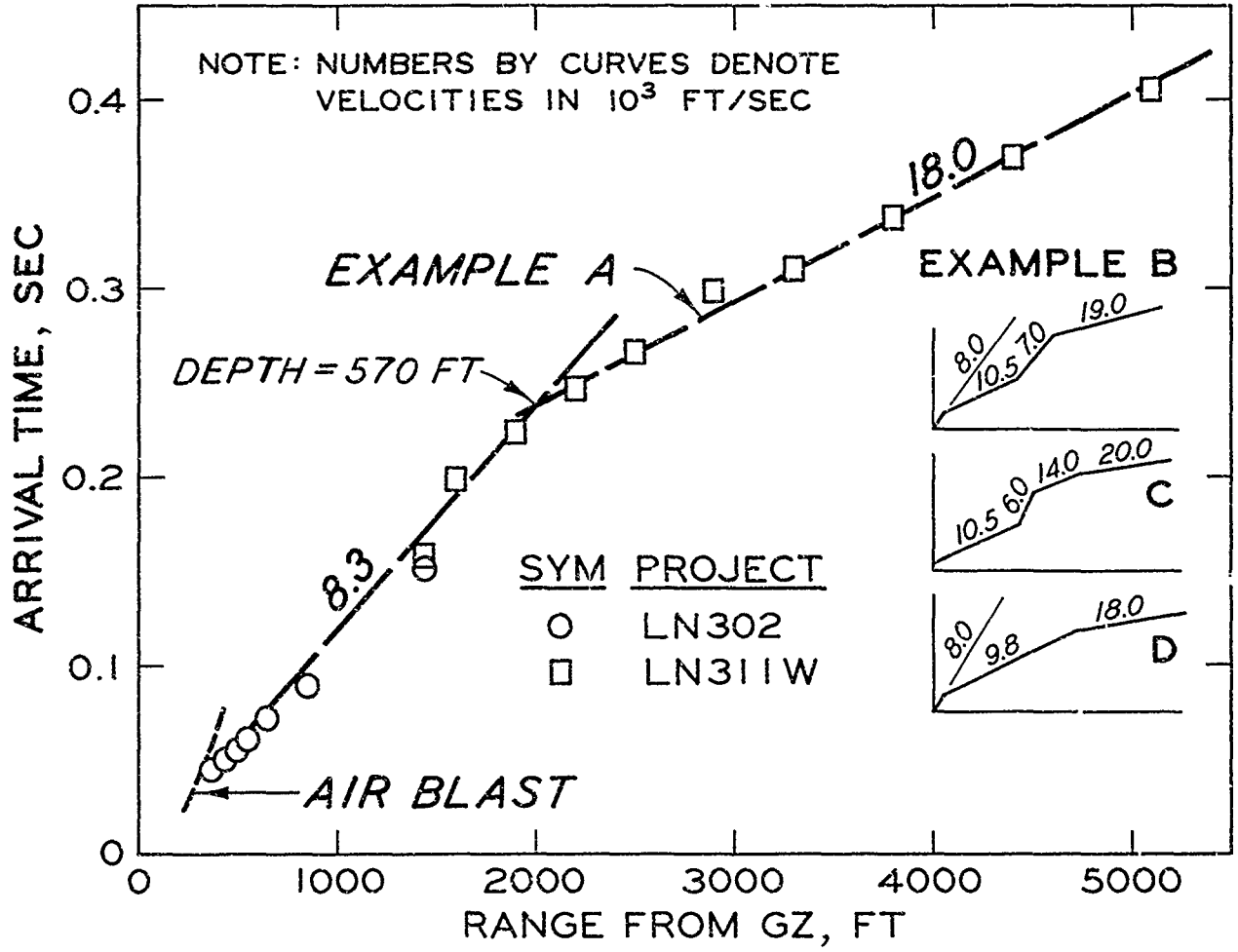

Figure 6 Arrival time of first motion versus range along the WES gage lines, with possible interpretations in terms of refracted seismic velocities.

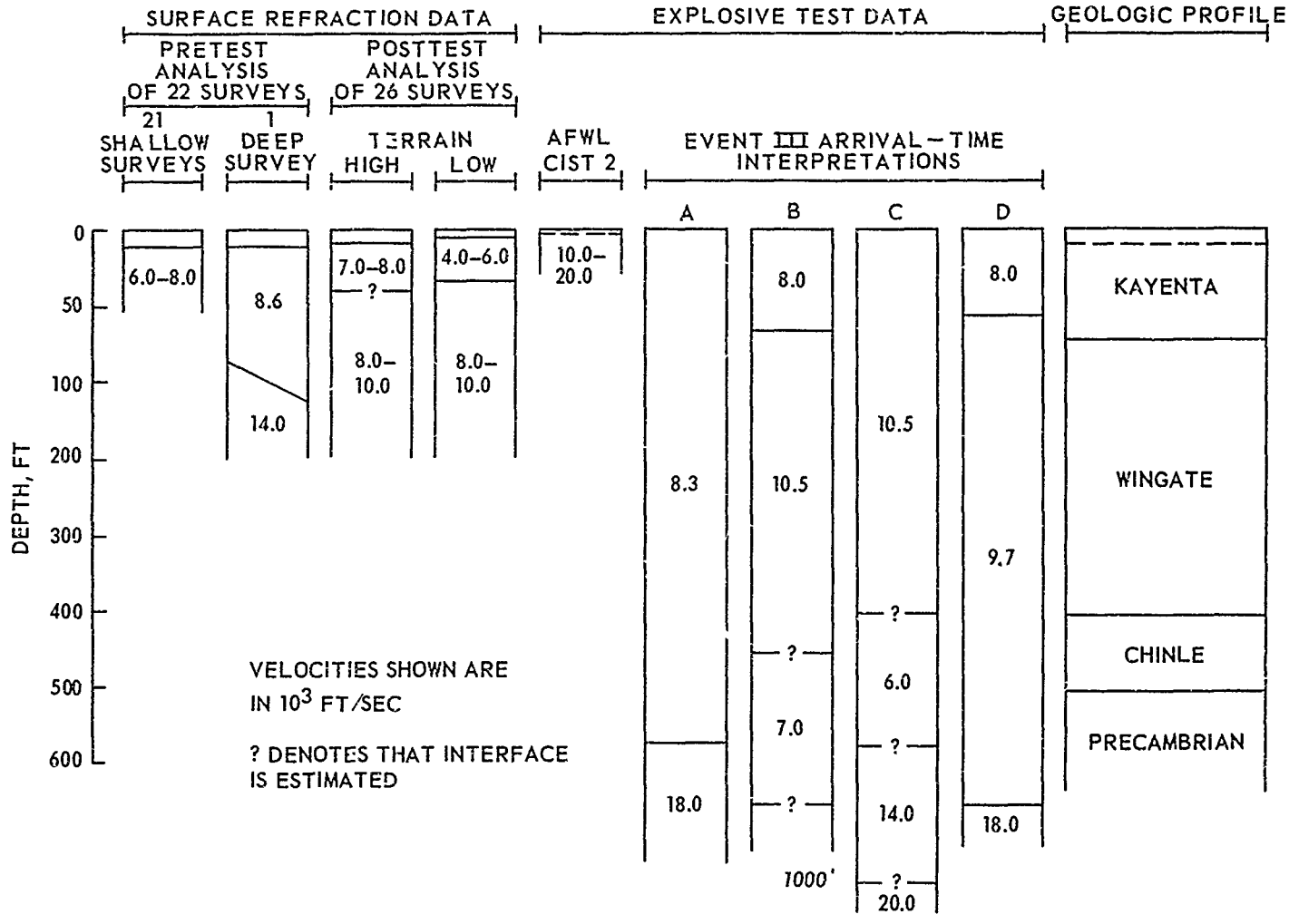

Figure 7 Summary plot of seismic velocity profiles in Mixed Company rocks (based on interpretations of various data) compared with estimated geologic profile.

CHAPTER 4

CONSTITUTIVE PROPERTIES

The constitutive or mechanical properties recommended for use in preshot ground motion predictions were selected so as to be compatible with other assumed properties, such as water content and seismic velocity. Obviously now, if the original assumptions regarding water contents and seismic velocities have been modified, the associated stress-strain and shear strength relationships must be modified. The mathematical constitutive model formulations employed in the preshot calculations were based on the assumption of loading-rate-independent and isotropic material behavior. It was also assumed that the laboratory test results were representative of in situ properties, and, in some cases, extrapolations of the available data were necessary in order to specify behavior at pressures above the range of laboratory test values. The purposes of this chapter, therefore, are to examine new data that bear on these assumptions and suggest possible modifications to the preshot property recommendations.

4.1 EFFECT OF WATER CONTENT CHANGES

At the time of Event III, the surface soil at the site was influenced by wet weather and construction conditions. As a result, it was recommended in Chapter 2 that the 5-foot-thick soil overburden layer originally specified be subdivided into two layers. The water content of the upper soil layer was estimated to be approximately 15 percent, while that of the lower layer was estimated to be about 7 percent. A series of UX tests were conducted on both undisturbed and remolded specimens obtained from the site on the day after the event. As expected (Reference 9), those specimens with 15 percent water content were initially more compressible than those with 7 percent water content, i.e., their initial UX response was probably dominated by intergranular friction, which increases as water content decreases. On the other hand, the specimens with increased water content contained fewer air voids than did the drier specimens, which caused them to stiffen or "lock up"

at smaller strains as these voids closed under the applied stresses. Figure 8 shows a plot of the recommended UX relations developed for the two soil layers (Layers 1A and 1B); an alternate layer (Layer 1C) for the composite 0- to 5-foot depth is also given for use in the event that the calculational grid cannot be designed to accept the two-layer representation.

The TX failure envelopes were significantly affected by the changes in water content. Test data from remolded specimens with 15 percent water content gave failure envelopes that achieved limiting or maximum principal stress difference values on the order of 300 to 500 psi under mean normal stresses greater than about 500 psi. The failure envelopes derived from tests on specimens with only 7 percent water content indicated a 6,500-psi limiting value for applied pressures on the order of a kilobar or greater. New yield surfaces and UX stress paths were developed for the two soil layers as a result of these changes in the shear strength profile.

4.2 EFFECT OF SEISMIC VELOCITY CHANGES

The initial uniaxial strain modulus M_i is assumed to be directly related to the seismic P-wave velocity v_p and the mass density ρ in the relation $M_i = \rho v_p^2$. Values of M_i were thus recalculated for all of the site materials using the revised seismic velocity and density values given in Tables 2 and 1, respectively. Because all of the dynamic UX test data indicated relatively low or soft initial moduli, it was assumed that the extremely stiff seismic moduli applied only for very low stress levels that were below the resolution of the UX test measurements, e.g., less than 10 psi for the Kayenta Formation materials. Although analyses of the data are still incomplete, the general consensus at the Mixed Company Project Review Meeting, held in March 1973, was that the maximum amplitudes of signals traveling with seismic velocity through this formation in both the AFWL CIST experiment and Event III were significantly larger, i.e., on the order of 200 psi.

Whereas the data from dynamic UX tests on unweathered Kayenta sandstones did not reveal a significant region of stiff, seismic

velocity-associated moduli, data from high-pressure (5-kbar and above) gun tests conducted by both WES and the Stanford Research Institute (SRI) certainly appear to indicate that moduli of this magnitude extend to stress levels very much above 200 psi. A comparison of the data from the two types of tests is shown in Figure 9. Assuming that both of these sets of laboratory data as well as both sets of field data are correct, one possible explanation for the wide variation in the stress levels associated with th stiff initial loading moduli is that this seismic "precursor" variance is due to loading-rate effects. Figure 10 shows a comparison of the loading times versus peak stress for laboratory static UX tests, dynamic UX tests, and high-pressure gun tests with those estimated from the CIST and Event III field data. The order of the data is certainly consistent with the loading-rate hypothesis.

To examine the effect of loading rate on initial uniaxial strain response, plots of stress/strain and stress/time from five dynamic UX tests on similar unweathered Kayenta material were enlarged as shown in Figure 11. Three of the five specimens had a stiffer initial response than the other two, but at axial stresses above about 20 psi, the constrained moduli from all five specimens were essentially the same (Figure 11a). Figure 11b shows that the stress pulses applied to these specimens had different initial loading rates, i.e., 2,000 to 3,000 psi/sec for Pulse 1 as opposed to 6,000 to 7,000 psi/sec for Pulse 2; at 20 psi, the loading rates for both pulse types increased to about 30,000 psi/sec. Above 20 psi, the rates appeared to continue to increase identically. The data in Figure 11 are admittedly too limited to warrant a positive confirmation, but like the data in Figure 10, they certainly tend to corroborate the loading-rate hypothesis.

Under field loadings, stresses in the superseismic region probably rise more uniformly to peak intensity, i.e., there is no slow lead-in. Therefore, because of the relatively slow lead-in characteristics of the laboratory loading pulses, the UX test specimens may not have been loaded fast enough initially to be representative of field conditions, and hence, the seismic-associated stress levels assumed for the pretest property recommendations would have been too low. From the above

reexamination of the available laboratory data, it now appears that a lower bound value of 50 psi is more reasonable for the stress level associated with seismic velocity. When the properties derived from the AFWL analysis of the CIST field data become available, they may give a better indication of the actual maximum stress level associated with the seismic speeds. However, it is possible that CIST-derived data might be an upper limit, since the loading rates in that experiment are considerably faster than those in Event III, except perhaps in the immediate vicinity of GZ.

4.3 EFFECT OF HORIZONTAL-TO-VERTICAL ANISOTROPY

It was obvious from the presence of bedding planes that response of the Kayenta rocks would be governed to some degree by anisotropic properties. Data from direct pull and Brazil tension tests confirmed that these materials have a substantially higher tensile strength in the horizontal direction than in the vertical direction (Reference 1). Unconfined compression (UC) tests were conducted by Terra Tek, Inc. (TT), on core with bedding planes oriented parallel and perpendicular to the loading axis (Reference 10). Strengths from the parallel oriented tests were as much as 50 percent lower than those obtained from perpendicularly oriented tests.

Recent compressibility data from WES UX tests on Kayenta sandstone specimens, some of which contained thin clay seams or beddings and some of which were uniform, are shown in Figure 12. As expected, the uniform specimens were less compressible; their responses to horizontal or vertical loadings were essentially the same. On the other hand, vertically oriented specimens containing horizontal clay seams were much more compressible than the horizontally oriented test specimens. Since the tests were limited to the relatively competent unweathered sandstones of the Kayenta formation, nothing is known as yet about the anisotropic compressibility characteristics of other materials, such as the weathered siltstone.

As previously indicated, the codes used in the pretest ground motion prediction calculations employed isotropic material models.

Therefore, even though the laboratory data obtained for the Mixed Company sandstones definitely indicate anisotropic stress-strain and tensile strength characteristics, a basic problem still remains as to how to utilize this information in specifying "effective" isotropic property values for subsequent calculations.

4.4 RECENT IN SITU AND LABORATORY STRENGTH DATA

One of the pretest analysis assumptions was that the then-available laboratory test data on Kayenta rock specimens were representative of in situ properties, since the Rock Quality Index of the core was greater than 90 percent and no other data existed that could be used to adjust the laboratory data to reflect in situ conditions. More recently, however, a UC test was conducted by TT at a rock outcrop near the CIST experiment on a large block of in-place sandstone (Reference 10). Corresponding laboratory tests were also conducted on this sandstone. The field strength was approximately 30 percent lower than the strength from similarly oriented, small-size laboratory specimens of the same sandstone. In the absence of comparative data on confined specimens, it is assumed that the unconfined results represent an upper-bound reduction factor, i.e., in situ and laboratory test data should agree best when the materials are confined under large static overburden or dynamic live loadings.

Additional information supplied by Lawrence Livermore Laboratory (LLL) on one type of Mixed Company sandstone has direct bearing on the validity of the pretest failure envelope shapes at high pressures (Reference 11). Prior to the LLL tests, the only failure data available were the WES low-pressure results and those obtained by TT at confining pressures of 2 and 4 kbars (see solid circles in Figure 13). A nearly linear relationship was assumed as shown in the figure in order to extend the envelope beyond that range of pressure. The LLL data confirmed the earlier WES and TT results but not the assumed high-pressure envelope. Rather, they showed an extremely nonlinear envelope that substantially increased under confining pressures in excess of 4 kbars (see open circles in Figure 13).

LLL also determined the failure strengths of specimens that had been first hydrostatically loaded to 7 kbars and then unloaded to lower confining pressures prior to application of shearing stresses. Structural collapse apparently occurred under the 7-kbar preloading since the resulting failure envelope was nearly linear, similar to that expected for a dense sand (see crosses in Figure 13). Thus, the sandstone material could have two failure envelopes, depending on its loading history. Although such crushing could only occur under very intense pressures of the magnitude expected at ranges very close to GZ, it could affect the characteristics of wave forms propagating out from that region.

4.5 RECOMMENDED POSTSHOT CONSTITUTIVE PROPERTIES

The complete set of representative stress-strain and strength relations for Layers 1A through 7 is presented in Appendix A. They consist of UX axial stress-axial strain relations, UX stress paths for both loading and unloading, and TX failure envelopes. The recommended postshot profile and composition properties were presented in Table 1, and the revised seismic velocity values were given in Table 2.

As stated in Section 4.2, initial UX compression moduli were recalculated for all of the site materials using the revised seismic velocity values. Each of the UX relations for Layers 1A through 7 reflects these moduli (Appendix A). The constitutive properties for the two overburden layers reflect the effect of increased water in the surface layer; Layer 1A is initially more compressible, locks at a smaller axial strain, and has less strength than Layer 1B.

For the Kayenta materials (Layers 2, 3, and 4), the initial portions of the originally recommended UX curves were altered to reflect a 50-psi stress level associated with their seismic velocities. The new curves were then smoothly transitioned so as to merge into the previously recommended relations at a stress level of about 2,000 psi, such as shown in Figure 14. No changes were recommended for stress levels above 2,000 psi, primarily because of the uncertainty expressed in Section 4.3 as to how to utilize the various horizontal and vertical data

to specify "effective" or "average" isotropic property values.

The unconfined strength data for Layer 2 were reduced by 30 percent from the pretest envelope to account for differences between in situ and laboratory test conditions. The envelope was gradually merged back toward the values of the pretest envelope at higher mean normal stress levels. The principal stress difference levels associated with unconfined strength for Layers 3 and 4 were reduced by 20 percent for the same reason, and the yield surfaces were then merged back into the values of the pretest envelopes. As shown in Figure 15, such changes are almost trivial for envelopes depicting strong Coulomb-type initial response. More substantial changes were made at high stress levels (20 to 60 ksi mean normal stress) where the envelopes reflect the nonlinear shape previously observed by LLL (see Figure 13).

The posttest constitutive properties for the Wingate Formation, Layer 5, are the same as the pretest properties with the exception that the initial portion of the UX curve has been modified to reflect the 50-psi seismic precursor. The remaining Chinle and Precambrian materials (Layers 6 and 7) are assumed to be elastic, with both sets of properties reflecting the revised compression wave velocities of 11,000 and 18,000 ft/sec, respectively.

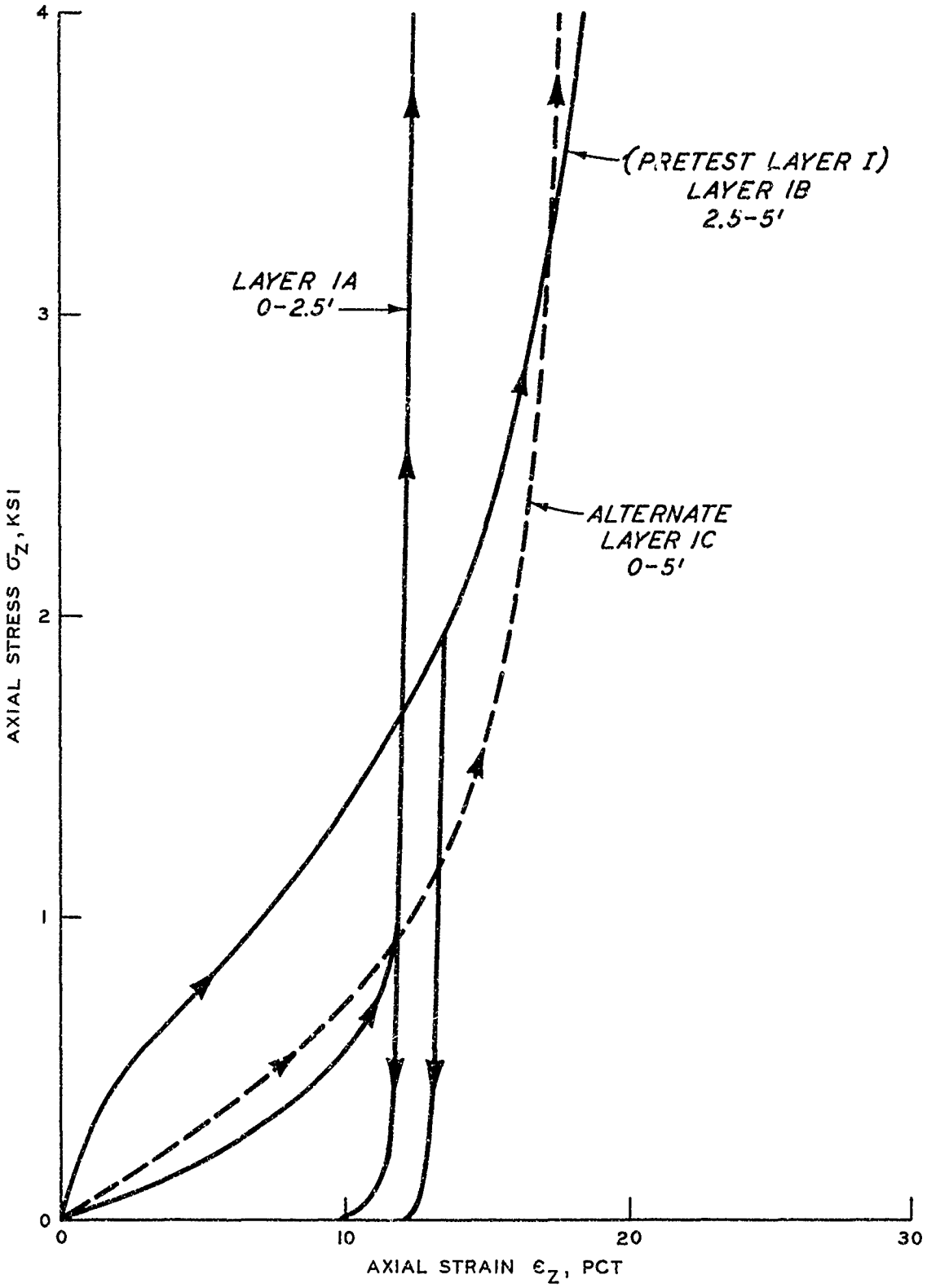

Figure 8 Recommended UX relations for Layers 1A, 1B, and alternate Layer 1C.

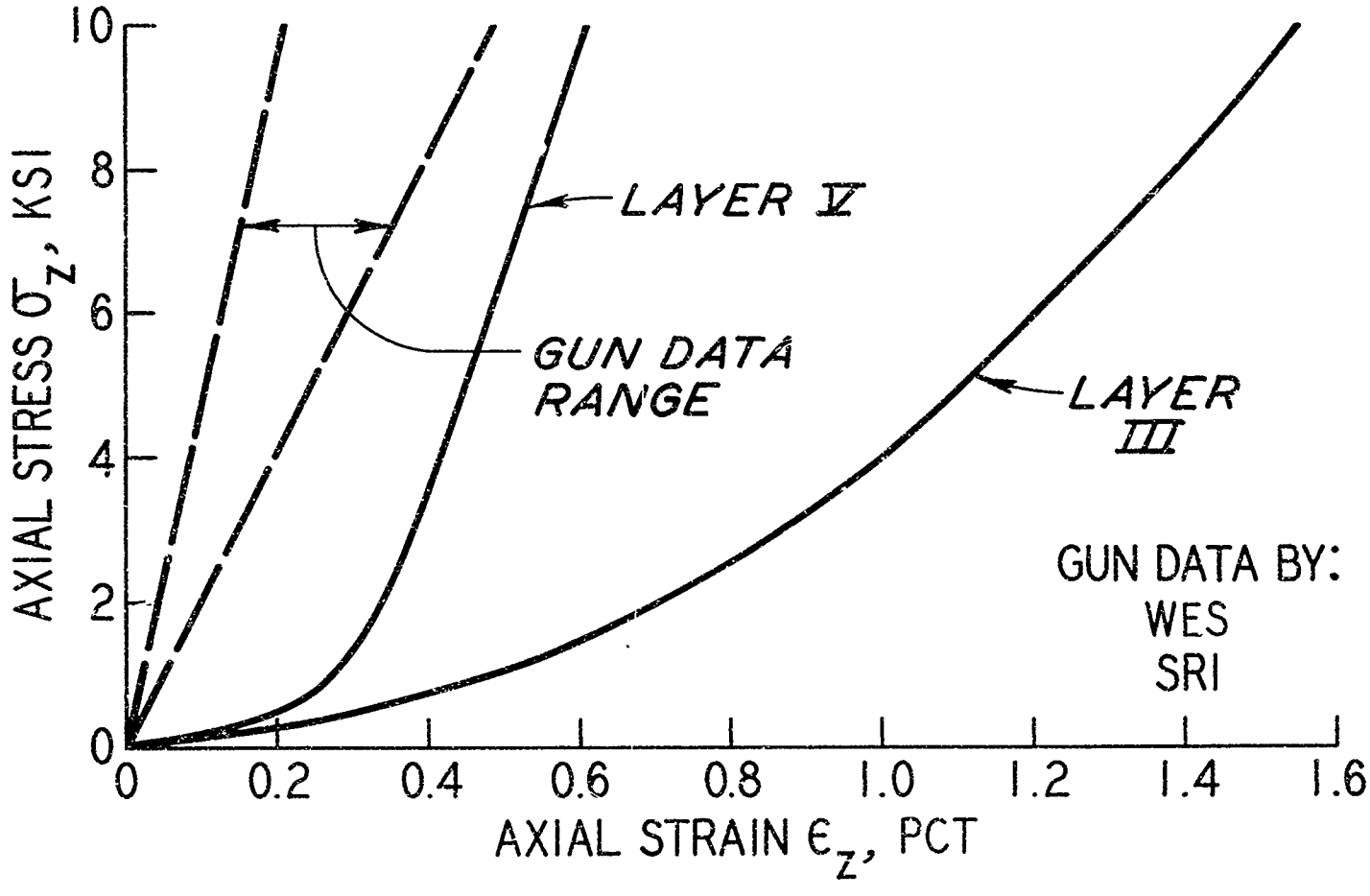

Figure 9 Comparison of pretest recommended UX relations for unweathered Kayenta sandctone with gun data.

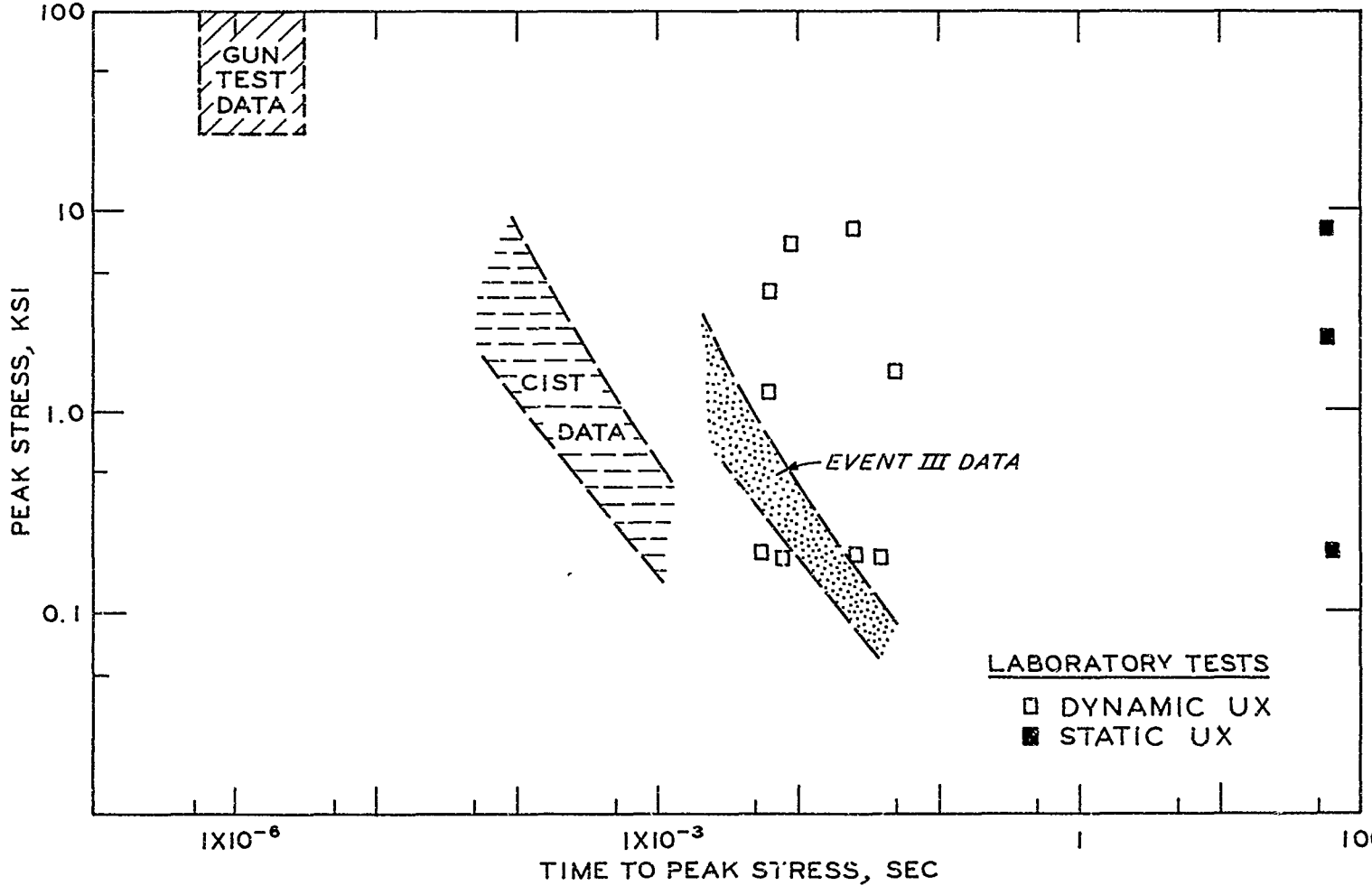

Figure 10 Comparison of loading times versus peak stress for laboratory tests with those estimated from field test measurements.

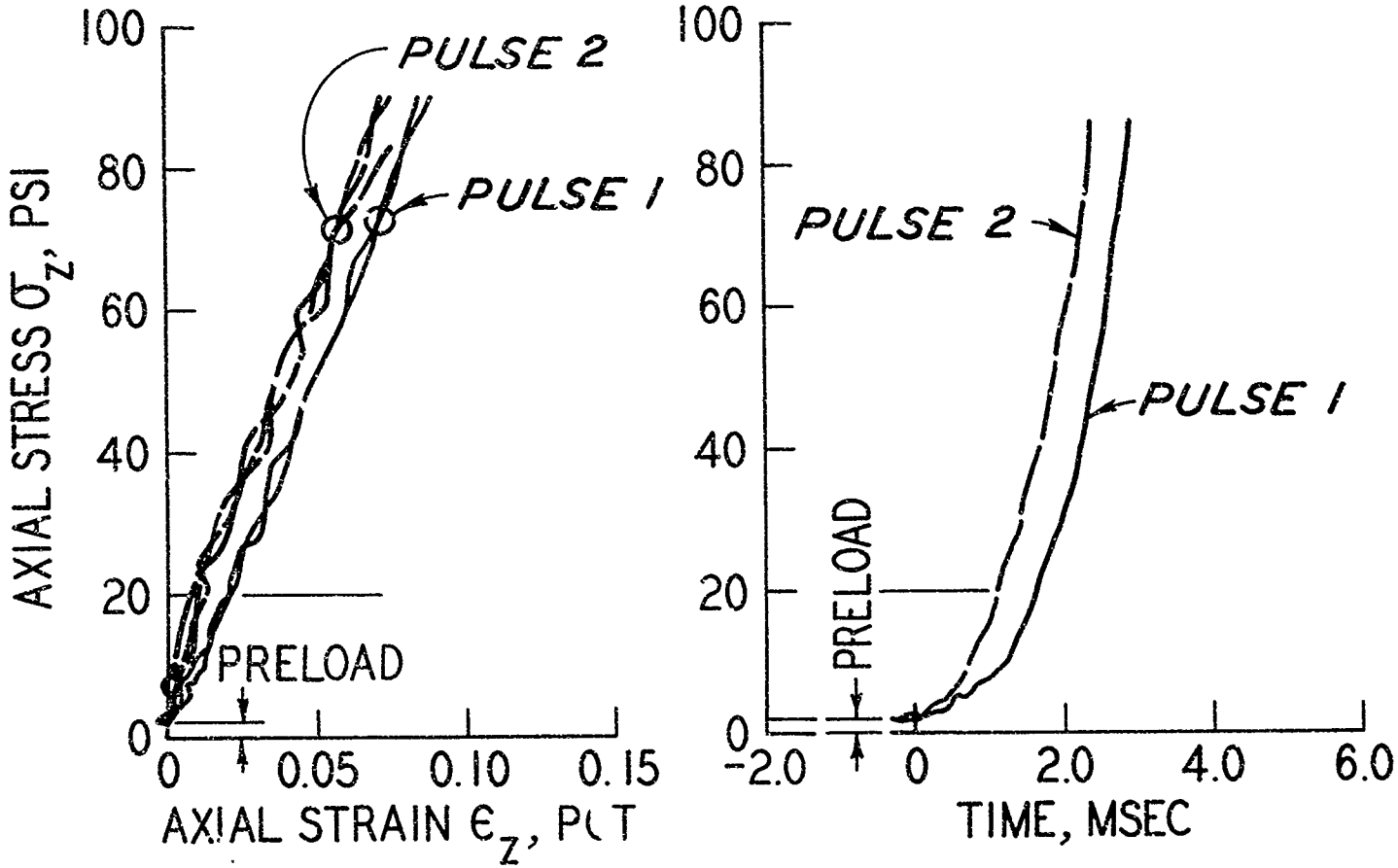

a. Plots of axial stress versus axial strain indicating initial material response.

b. Plots of axial stress versus time indicating initial loading history.

Figure 11 Enlarged plots of dynamic UX test data from five specimens of unweathered Kayenta sandstone.

TEST	TYPE SANDSTONE	ORIENTATION	LOADING RATE
1 S	UNIFORM	HORIZ	STATIC
2S	UNIFORM	VERT	STATIC
3D	CLAY SEAMS	HORIZ	DYNAMIC
4D	CLAY SEAMS	HORIZ	DYNAMIC
5D	CLAY SEAMS	VERT	DYNAMIC
6D	CLAY SEAMS	VERT	DYNAMIC

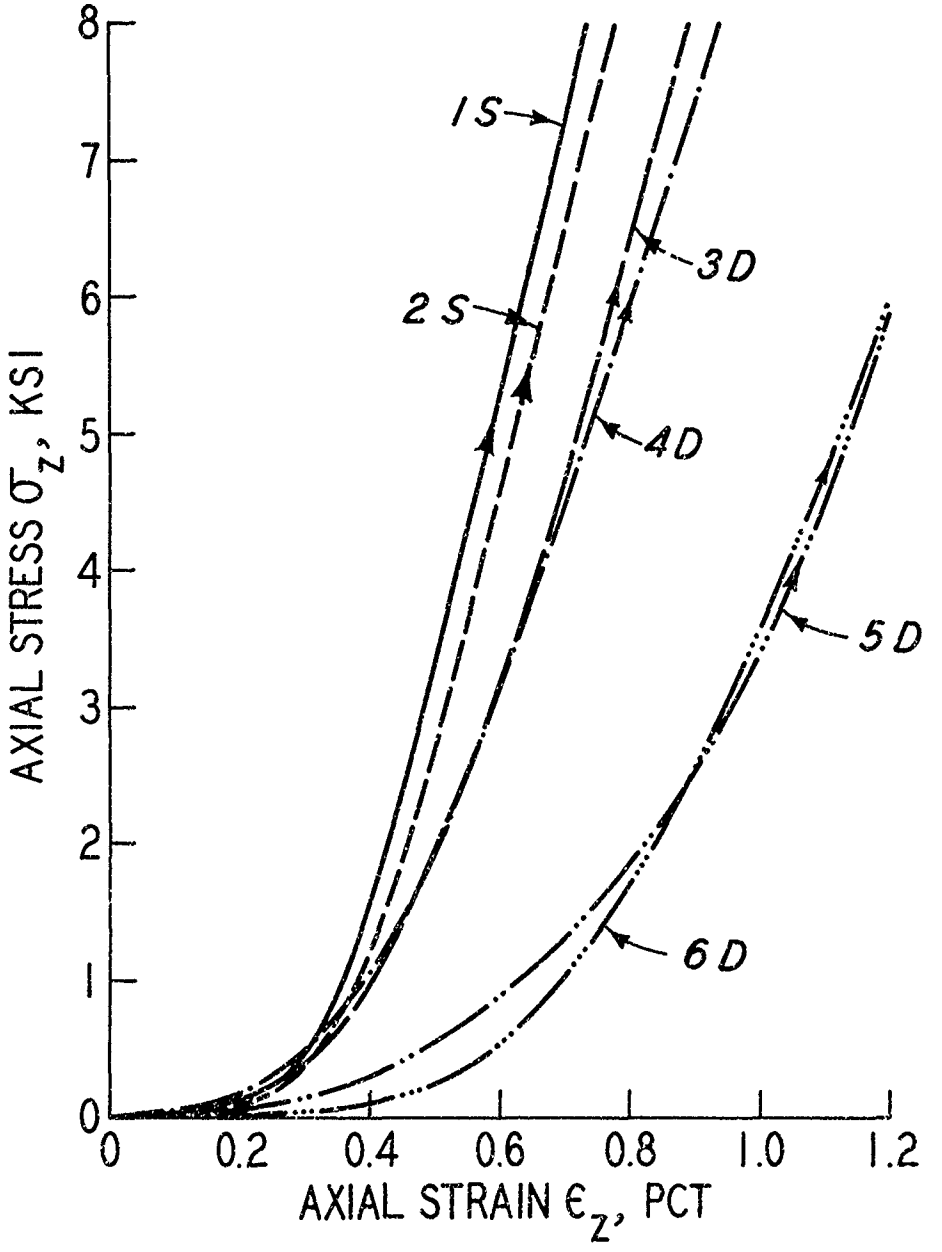

Figure 12 Results of horizontally and vertically oriented UX tests on uniform Kayenta sandstone specimens and specimens with clay seams.

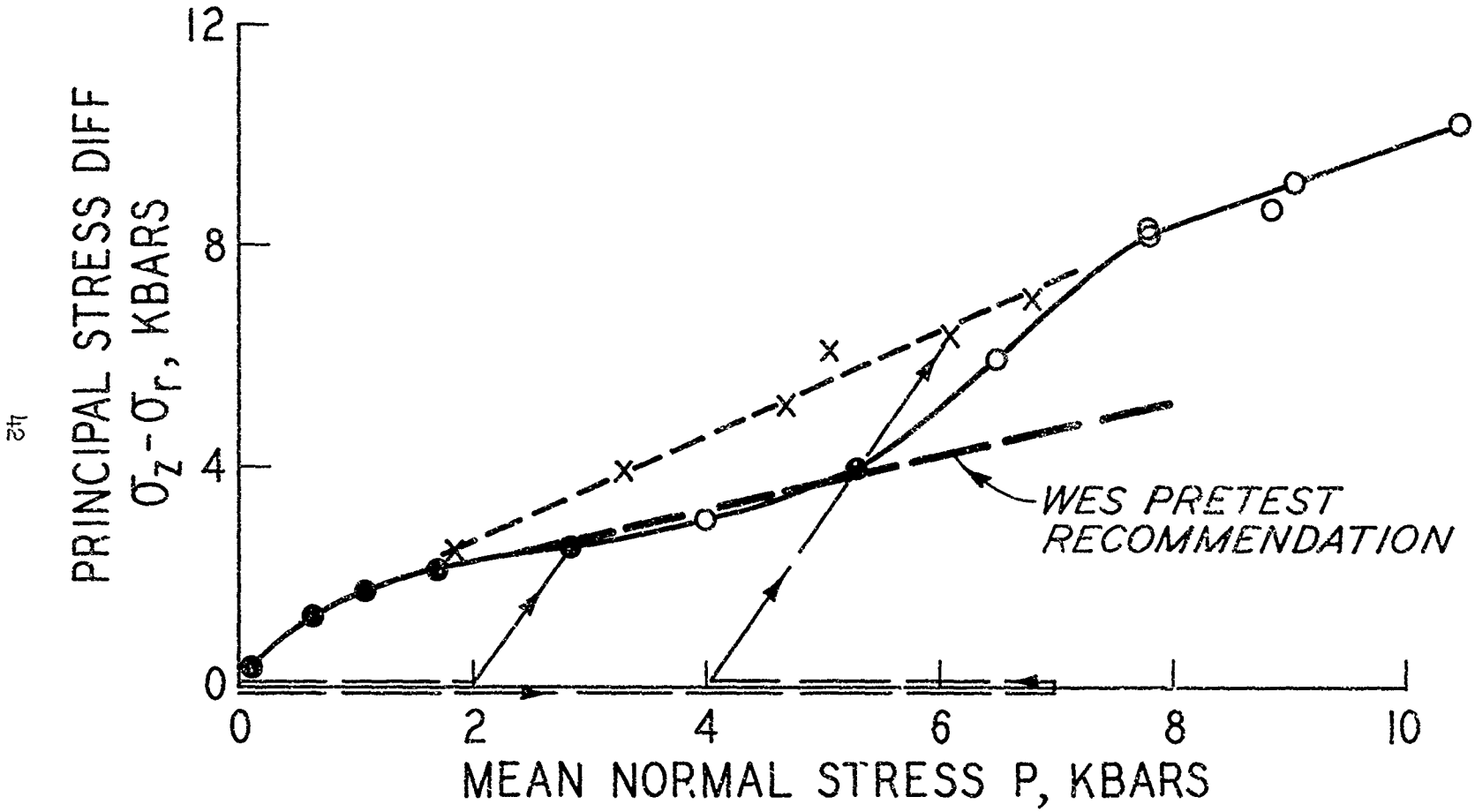

Figure 13 Preliminary results of TX tests by LLL on virgin specimens of Mixed Company sandstone (circles) and specimens previously subjected to 7-kbar hydrostatic confinement (crosses).

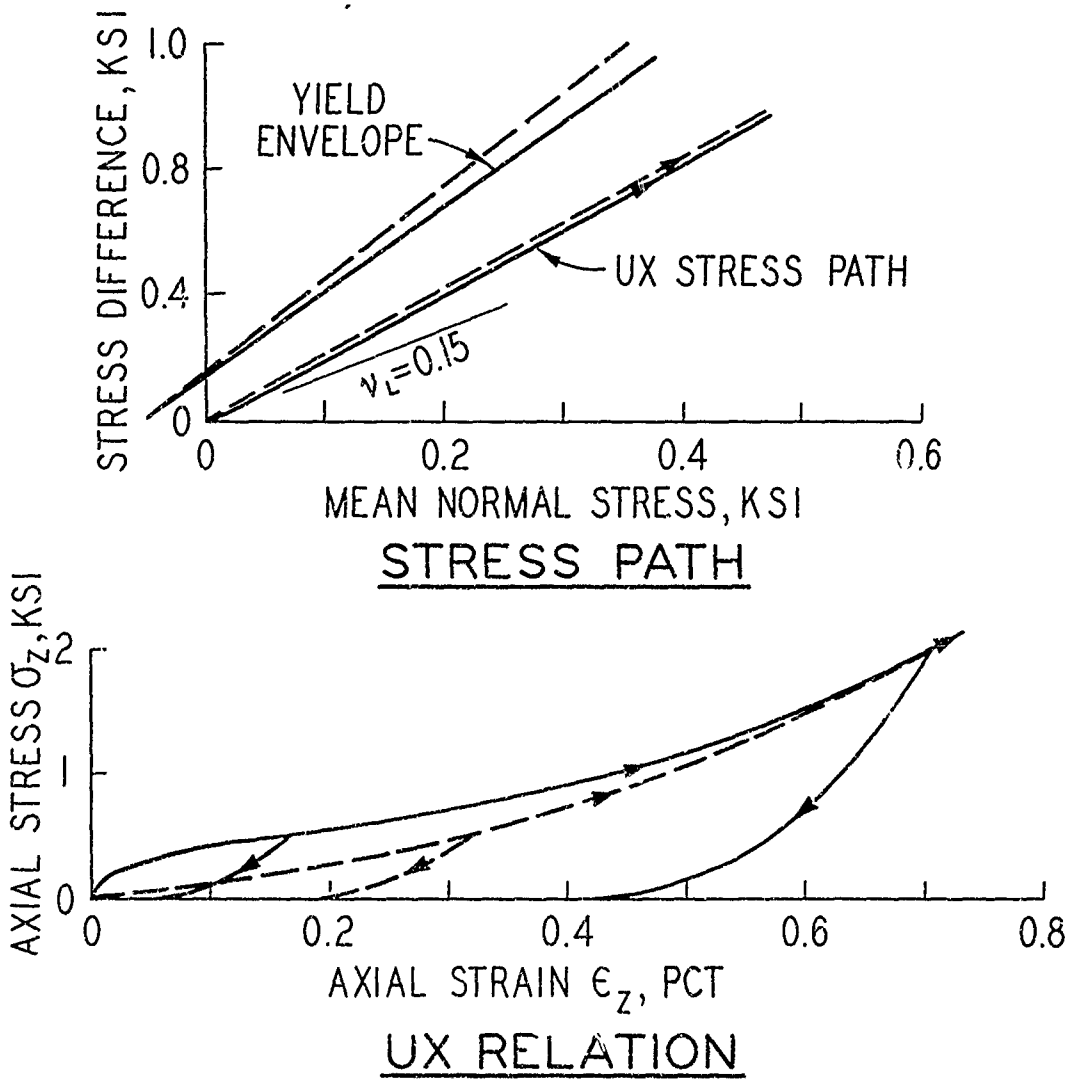

Figure 14 Comparison of UX loading and unloading relation recommended for posttest Layer 3 (solid lines) with relation recommended for pretest Layer III (dashed lines).

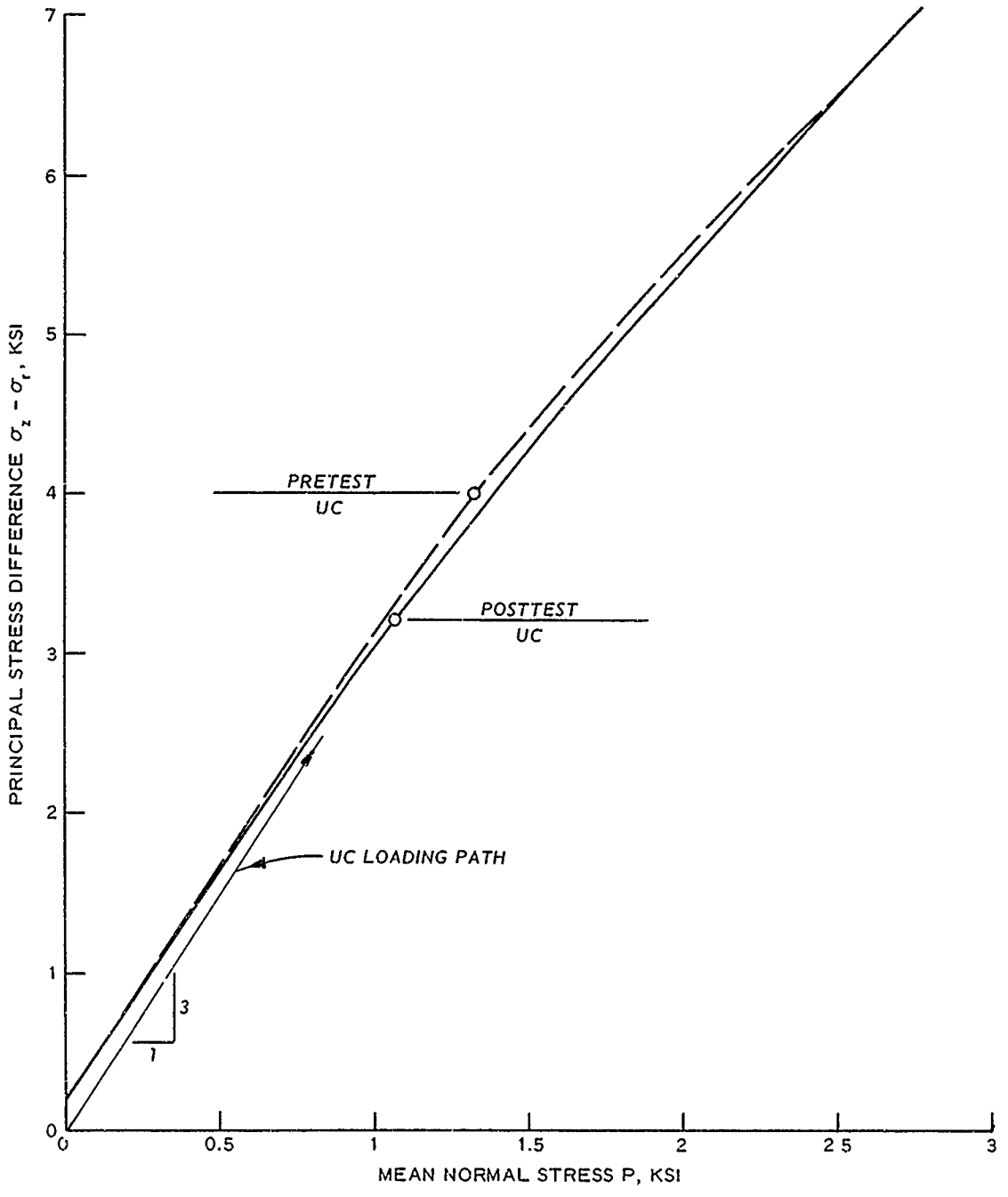

Figure 15 Comparison of low-pressure TX failure envelope recommended for posttest Layer 3 (solid line) with relation recommended for pretest Layer III (dashed line).

CHAPTER 5

CONCLUSIONS AND RECOMMENDATIONS

The pretest ground motion predictions did not agree very well with the ground shock measurements made during Mixed Company Event III. However, a number of invalidated assumptions were made in the process of developing the preshot profile and property idealizations. In addition, the mathematical models were hurriedly fit in order to make the pretest calculation and did not closely replicate all features of the recommended profile and properties. As a result, it was concluded that sufficient uncertainties existed to warrant: (1) a reevaluation of the profile and properties in the light of more recent data, and (2) a recalculation of Event III with a much more precise fit to the constitutive properties and profile resulting from this evaluation.

The pretest calculational grid extended only to a depth of about 300 feet, i.e., into the Wingate Formation. Examination of possible travel paths showed that signals reflected from the Chinle and Precambrian layers could have arrived in time to influence the ground motions measured during Event III. It is therefore strongly recommended that the grid used in any recalculation extend to depths of 500 to 600 feet, i.e., into the Precambrian basement.

Samples taken just a few days after the event showed that the wet weather conditions existing at shot time resulted in a significant increase in the water content of the upper 2 to 3 feet of the overburden soil over that determined earlier; tests on these samples showed that the increased water substantially affected the compressibility of these materials. It is now recommended that the postshot calculational zoning be set fine enough to accommodate an idealization of the overburden soil into two horizontal layers, rather than into one as orginally recommended for preshot calculations.

With the uncertainties surrounding the definition of seismic velocities and constitutive properties, it appears that the most practical approach at this time would be to keep the profile for the planned recalculation as simple as possible. Thus, it is recommended that the

4-foot-thick artificial layer, which was included in the preshot profile to represent the soft clayey conglomerate material occurring randomly throughout the Kayenta Formation, be eliminated from the postshot profile. However, the basic assumption of lumping small zones of material, which cannot be incorporated in the profile due to computational grid-size limitations, into one or more larger layers should be evaluated in future parametric studies.

An extensive reanalysis of the available surface refraction survey data along with analysis of the Event III ground motion data resulted in revisions to the seismic velocity profile as listed in Table 2. Horizontal velocities measured by AFWL in its CIST experiment could not be reconciled with the refraction survey data; a cross-hole seismic survey is definitely recommended to assist in resolving this uncertainty.

Based on the data and analyses presented herein, new constitutive property recommendations have been developed for each of the layers in the proposed postshot profile (Appendix A). Values of initial UX moduli were recalculated for all of the site materials using the revised seismic velocity values. The stress levels associated with these moduli were originally assumed to be quite low, e.g., less than 10 psi for the Kayenta Formation materials. A lower bound value of 50 psi is now recommended as being more reasonable for the initial Kayenta "precursor" stress. This phenomenon appears to be a function of loading rate and definitely requires further study.

Tests on the Kayenta materials also revealed that horizontal-to-vertical anisotropy undoubtedly affected the ground motion results. But the problem of how to utilize the various horizontal and vertical data to specify meaningful "effective" or "average" isotropic property values still remains as a nagging item for further research.

In the preshot analysis, yield envelopes were extended in relatively simple linear fashion to pressure ranges beyond that of the pretest data. As a result of recent LLL data, substantial changes have been made in the failure envelopes, which now reflect a highly nonlinear behavior, including significant strength increases at high pressures.

Care should be taken in fitting the material models for the

proposed postshot calculation in order to insure that they reflect the revised properties as closely as possible. Recent developments related to cap-type constitutive models have significantly improved their ability to mirror detailed and complex material property specifications. If after doing this the recalculated ground motions still do not reasonably match the field data, attention should be directed toward defining properties and developing simplified models for loading-rate-dependent and/or anisotropic materials.

REFERENCES

1. J. Q. Ehrgott; "Preshot Material Property Investigation for the Mixed Company Site: Summary of Subsurface Exploration and Laboratory Test Results"; paper presented at Mixed Company/Middle Gust Project Review Meeting, 13-15 March 1973; Santa Barbara, Calif.; Unclassified.

2. I. S. Sandler, J. P. Wright, and M. L. Baron; "Data Report, Pretest Ground Motion Calculations for the Mixed Company Event of the Middle North Series"; Contract Report, October 1972; U. S. Army Engineer Waterways Experiment Station, CE, Vicksburg, Miss.; prepared by Weidlinger Associates, Consulting Engineers, under Contract No. DACA 39-72-C-0002 and DACA 39-70-C-0016; Unclassified.

3. J. Q. Ehrgott; "Preshot Material Property Investigation for the Mixed Company Site: Summary of Subsurface Exploration and Laboratory Test Results"; Miscellaneous Paper S-73-6, Tables 4.1 and 4.2, October 1973; U. S. Army Engineer Waterways Experiment Station, CE, Vicksburg, Miss.; Unclassified.

4. R. E. Leach; "Refraction Seismic Site Investigation at Site D, Grand Junction, Colorado"; Memorandum for Record, 4 October 1971; U. S. Army Engineer Waterways Experiment Station, CE, Vicksburg, Miss.; Unclassified.

5. Air Force Weapons Laboratory, Kirtland Air Force Base, N. Mex.; Letter to: U. S. Army Engineer Waterways Experiment Station, CE, Vicksburg, Miss.; Subject: "Transmittal of Data Package"; 19 January 1973; Unclassified.

6. J. K. Ingram; "Ground Motion and Stress, Project LN302"; paper presented at Mixed Company/Middle Gust Project Review Meeting, 13-15 March 1973; Santa Barbara, Calif.; Unclassified.

7. S. P. Chisolm, Air Force Weapons Laboratory, Kirtland Air Force Base, N. Mex.; Letter to: U. S. Army Engineer Waterways Experiment Station, CE, Vicksburg, Miss.; Subject: "Shock Front Profile, Project LN302a"; 26 April 1973; Unclassified.

8. R. F. Ballard, Jr., and R. E. Leach; "Project LN311W Strong Motion Seismic Measurements"; paper presented at Mixed Company/Middle Gust Project Review Meeting, 13-15 March 1973; Santa Barbara, Calif.; Unclassified.

9. A. J. Hendron, Jr., M. T. Davisson, and J. F. Parola; "Effect of Degree of Saturation on Compressibility of Soils from the Defence Research Establishment, Suffield"; Contract Report S-69-3, April 1969; U. S. Army Engineer Waterways Experiment Station, CE, Vicksburg, Miss.; prepared by M. R. Davisson, Foundation Engineer, under Purchase Order No. WESBPJ-68-67; Unclassified.

10. H. R. Pratt, Terra Tek, Inc., Salt Lake City, Utah; Letter to: Air Force Weapons Laboratory, Kirtland Air Force Base, N. Mex.;

Subject: "Progress Report on Contract F29601-72-C-0121"; 12 December 1972; Unclassified.

11. R. C. Heard, Lawrence Livermore Laboratory, Livermore, Calif.; Letter to: U. S. Army Engineer Waterways Experiment Station, CE, Vicksburg, Miss.; 5 April 1973; Unclassified.

APPENDIX A

REPRESENTATIVE STRESS-STRAIN AND STRENGTH RELATIONS

An idealized profile and set of constitutive properties were developed for use in the postshot calculation of the Mixed Company Event III test. The recommended postshot profile and composition properties are summarized in Table A.1 which lists the layer number, the material description, the depth range for each layer, the values of wet density, water content, and volume of air, the seismic velocity, and the tension limit (tension cutoff) of axial stress. The constitutive properties consist of a UX axial stress-axial strain relation, a principal stress difference-mean normal stress path for UX, and a TX failure envelope. The constitutive properties for Layer 1A are shown in Figures A.1 to A.4; Layer 1B properties, in Figures A.5 to A.10; Layer 2, in Figures A.11 to A.15; Layer 3, in Figures A.16 to A.19; Layer 4, in A.20 to A.23; Layer 5, in A.24 to A.26; and Layers 6 and 7, in Figure A.27. All of the properties reflect the response of the materials to live stress loadings. Tension cutoff values, including the contribution due to overburden stress, are indicated for layer interface locations, i.e., top and bottom of each layer.

TABLE A.1 SUMMARY OF POSTSHOT PROFILE AND COMPOSITION PROPERTIES FOR MIXED COMPANY ANALYSES

Layer Number	Material Description	Depth, ft		Wet Density pcf	Water Content pct	Volume of Air pct	Seismic Velocity ft/sec	Tension Limit of σ_z[a] psi
		From	To					
1A	Fill and/or top portion of overburden soil	0	2-1/2	120.1	15.5	11.7	1,300	$-(\gamma z)$
1B	Bottom portion of overburden soil	2-1/2	5	111.3	7.0	25.9	1,300	$-(\gamma z)$
1C	Composite of both fill and natural soil	0	5	116.5	12.0	17.5	1,300	$-(\gamma z)$
2	Weathered Kayenta material	5	9	137.0	3.5	12.8	3,500	$-(\gamma z)$
3	Upper 1/4 unweathered Kayenta material	9	24	145.0	4.5	6.4	8,000	$-(\gamma z + 15$ psi)
4	Lower 3/4 unweathered Kayenta material	24	70	147.0	4.5	5.1	10,000	$-(\gamma z + 100$ psi)
5	Wingate sandstone	70	400	128.4	7.0	14.0	8,000	$-(\gamma z + 80$ psi)
6	Chinle siltstone	400	500	158.0	--	--	11,000	$-(\gamma z + 40$ psi)
7	Precambrian basement rock	>500		162.0	--	--	18,000	$-(\gamma z + 700$ psi)

[a] σ_z = axial stress, γ = wet density, z = depth.

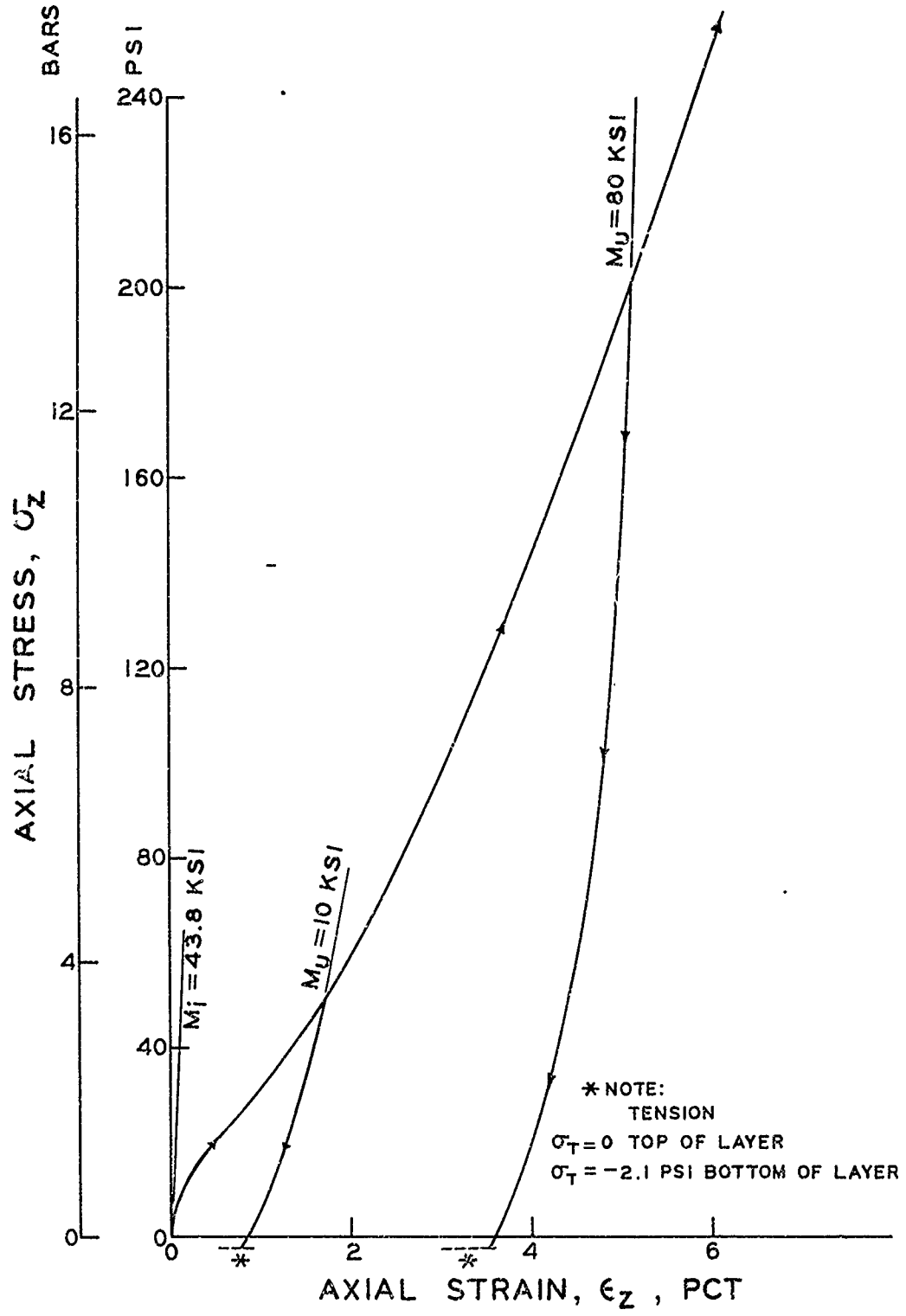

Figure A.1 Representative σ_z versus ϵ_z relation for uniaxial strain with unloading curves from σ_z = 50 and 200 psi for Layer 1A.

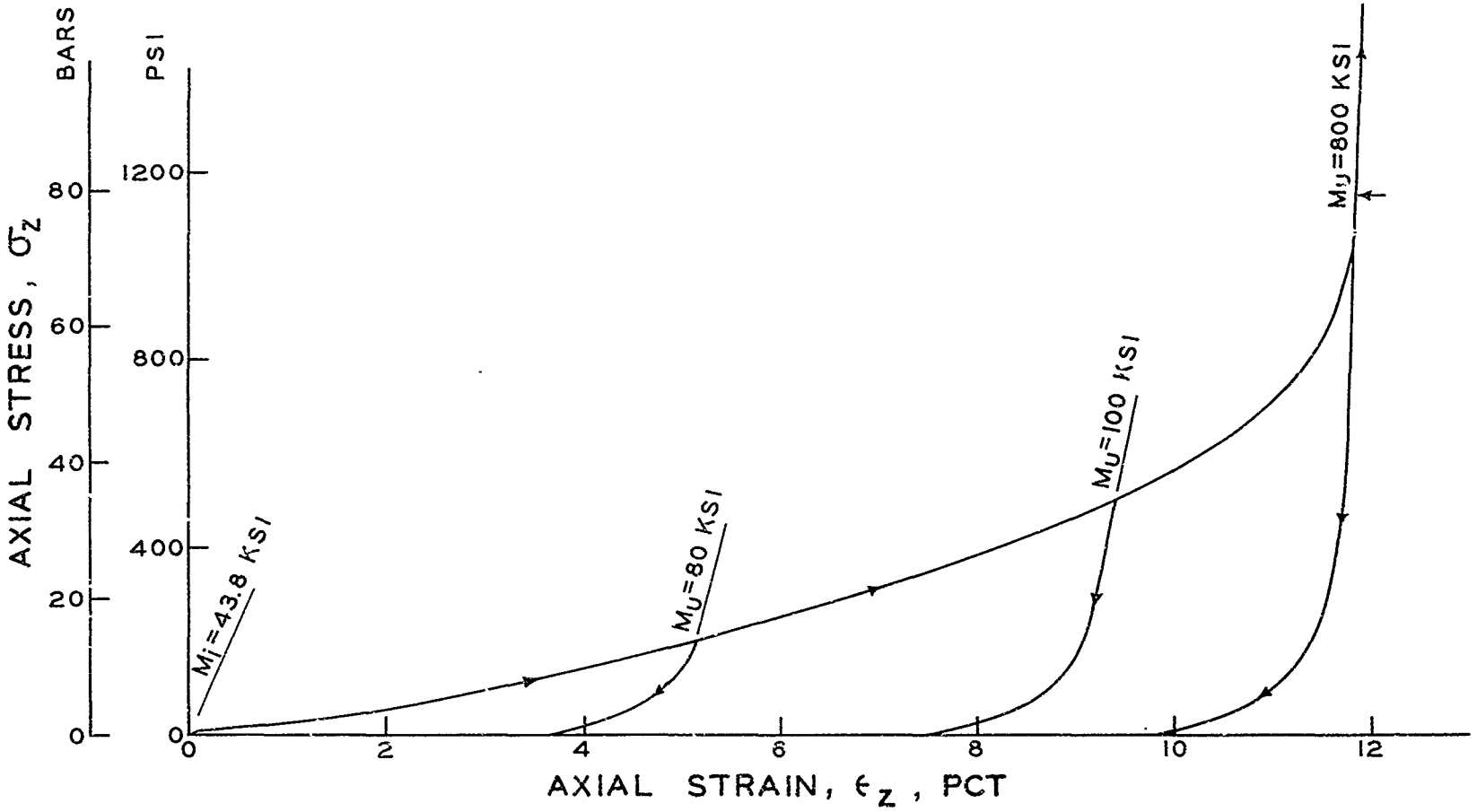

Figure A.2 Representative σ_z versus ε_z relation for uniaxial strain with unloading curves from σ_z = 200, 500, and 1,150 psi for Layer 1A.

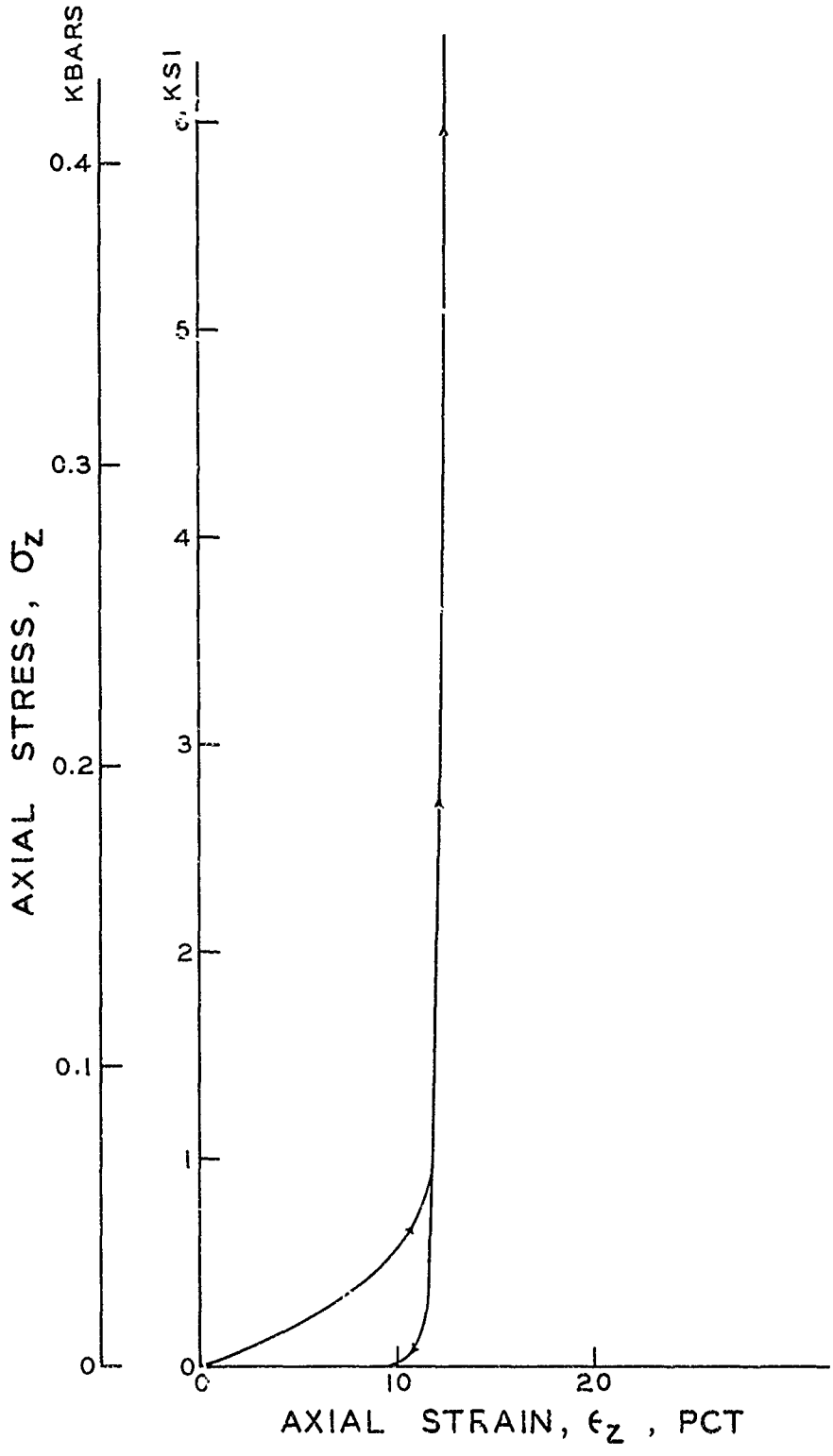

Figure A.3 Representative σ_z versus ε_z relation for uniaxial strain to σ_z = 6,000 psi for Layer 1A.

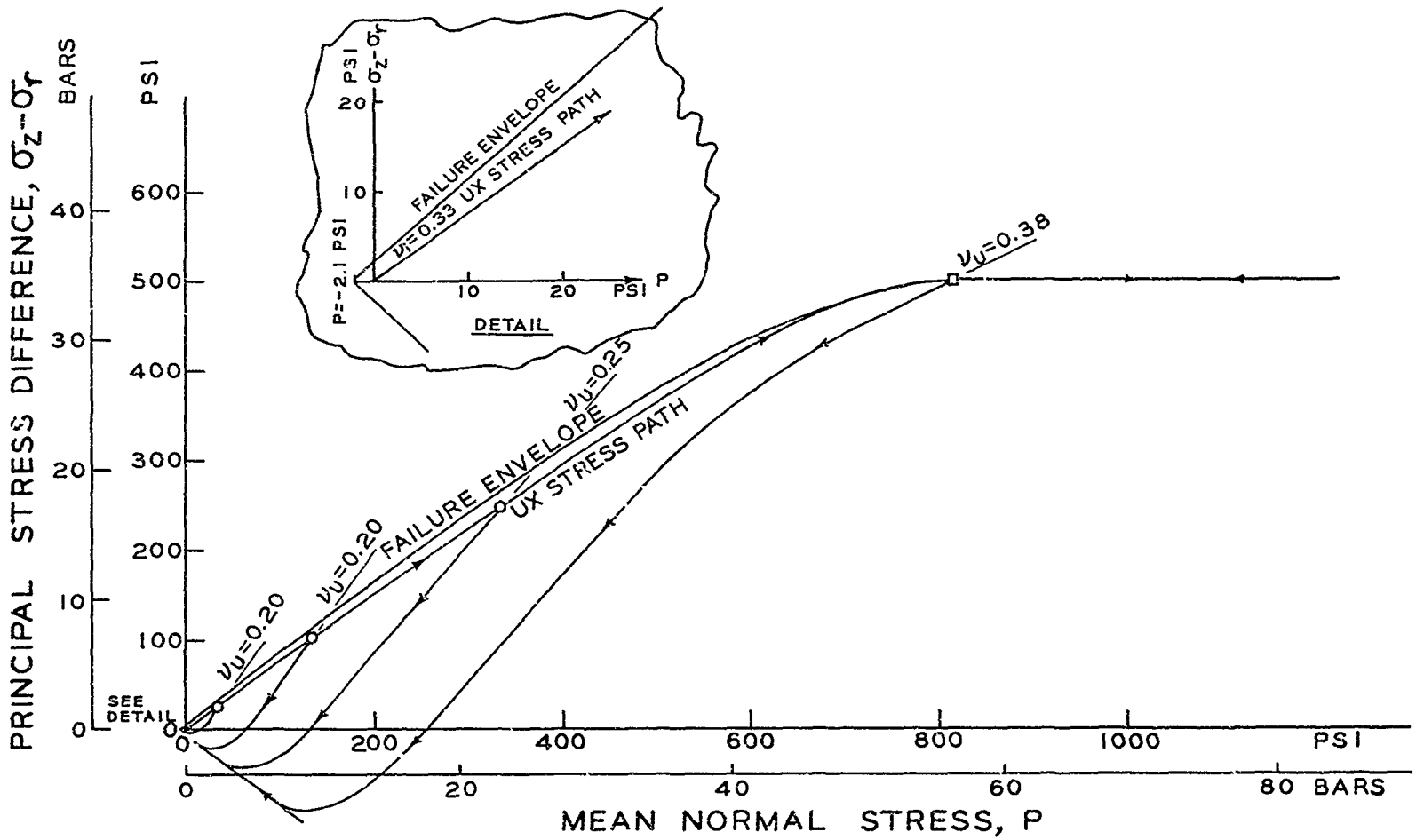

Figure A.4 Representative $(\sigma_z - \sigma_r)$ versus p stress paths for uniaxial strain and $(\sigma_z - \sigma_r)_{max}$ versus p failure envelope for triaxial shear to p = 1,200 psi for Layer 1A.

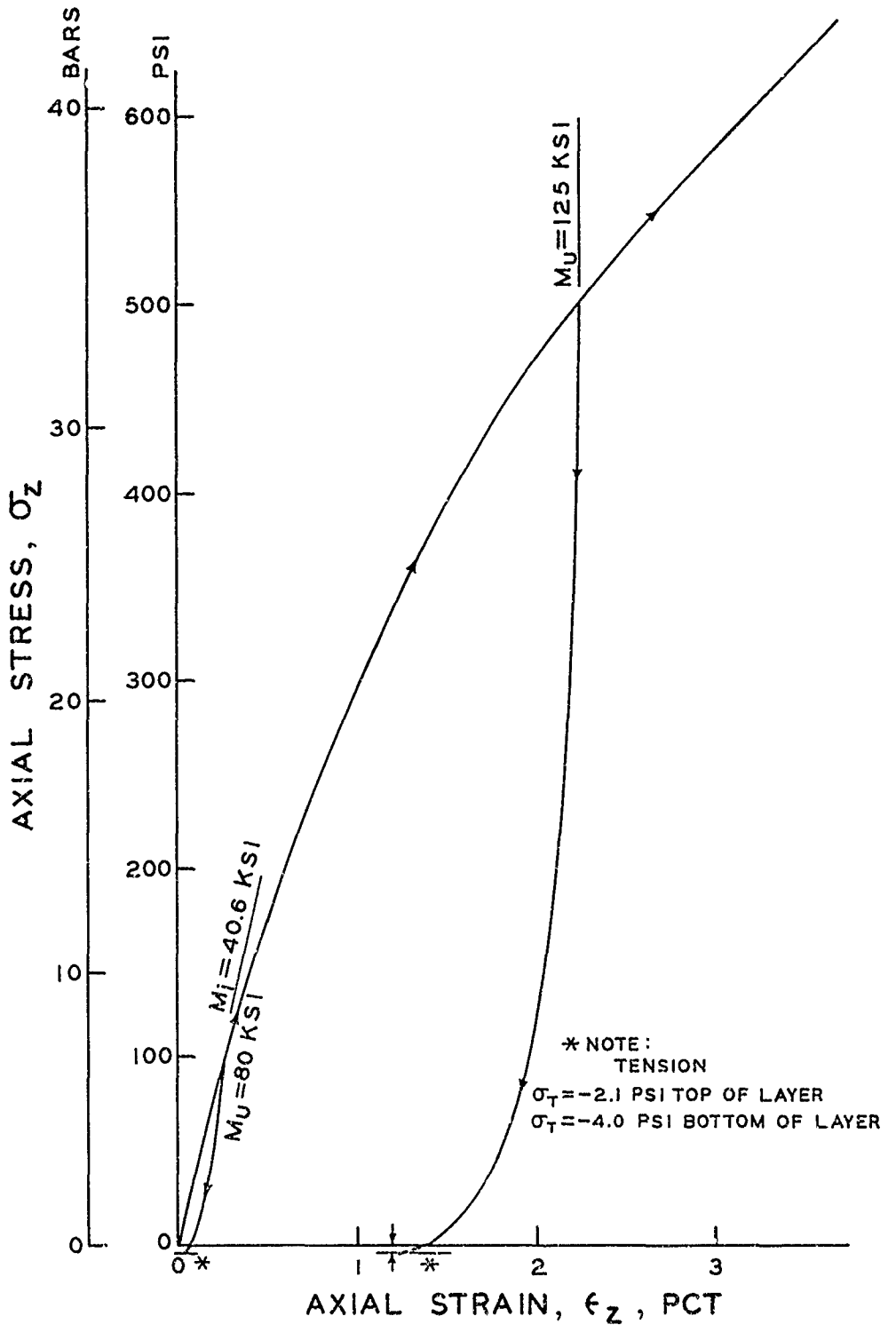

Figure A.5 Representative σ_z versus ε_z relation for uniaxial strain with unloading curves from σ_z = 100 and 500 psi for Layer 1B.

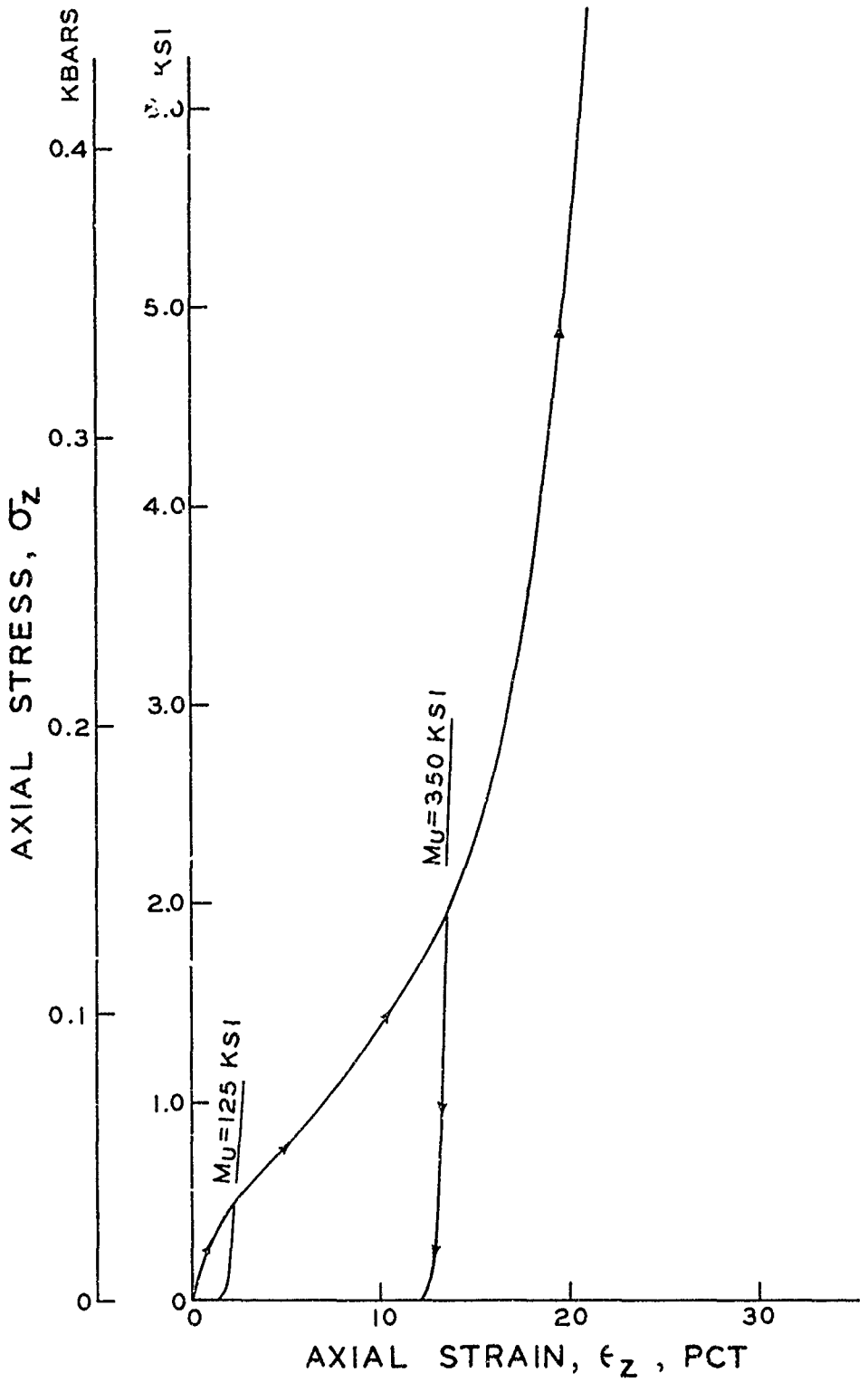

Figure A.6 Representative σ_z versus ε_z relation for uniaxial strain with unloading curves from σ_z = 500 and 1,950 psi for Layer 1B.

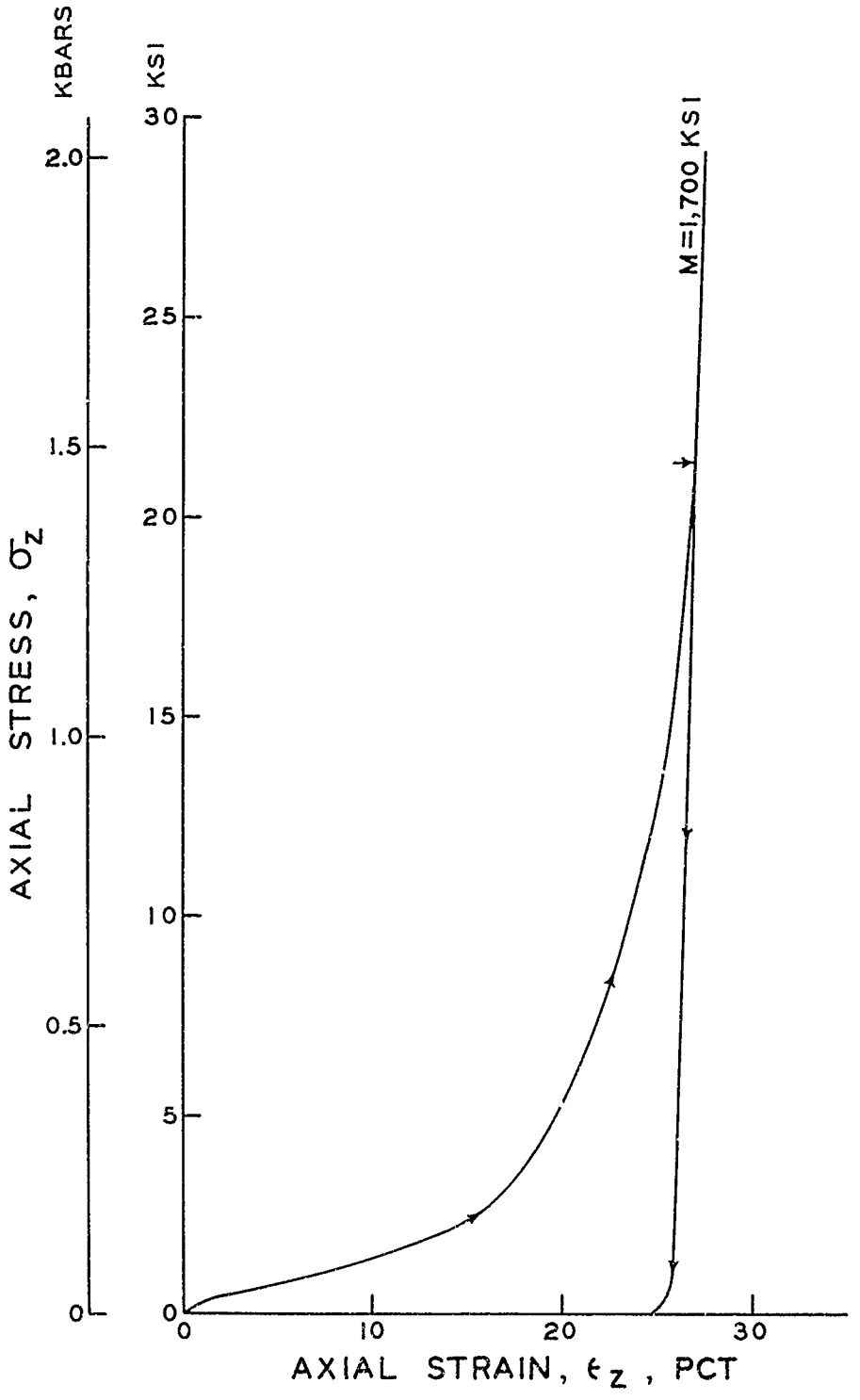

Figure A.7 Representative σ_z versus ϵ_z relation for uniaxial strain to σ_z = 30,000 psi for Layer 1B.

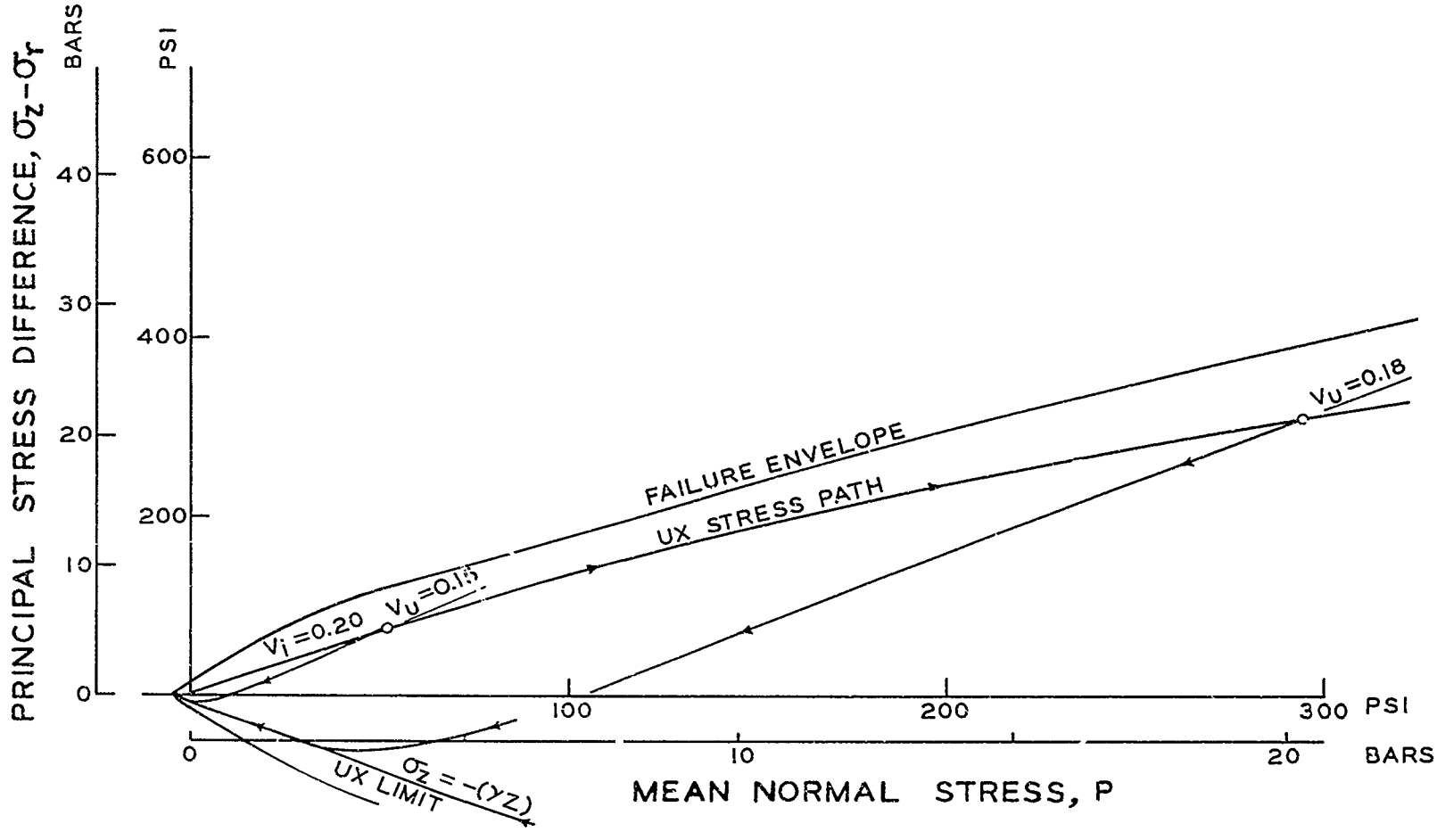

Figure A.8 Representative $(\sigma_z - \sigma_r)$ versus p stress paths for uniaxial strain and $(\sigma_z - \sigma_r)_{max}$ versus p failure envelope for triaxial shear to p = 300 psi for Layer 1B.

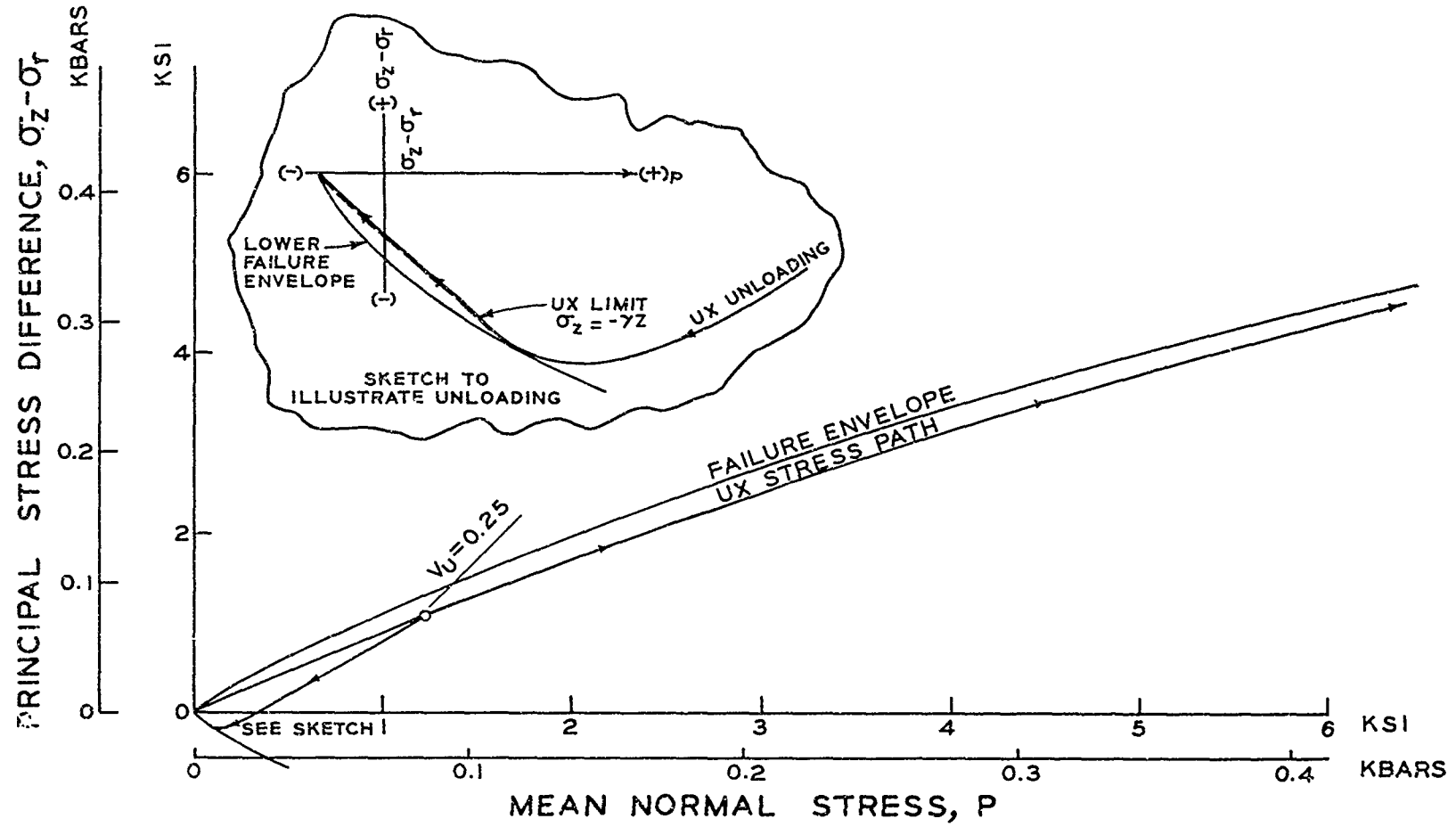

Figure A.9 Representative $(\sigma_z - \sigma_r)$ versus p stress path for uniaxial strain and $(\sigma_z - \sigma_r)_{max}$ versus p failure envelope for triaxial shear to p = 6,000 psi for Layer 1B.

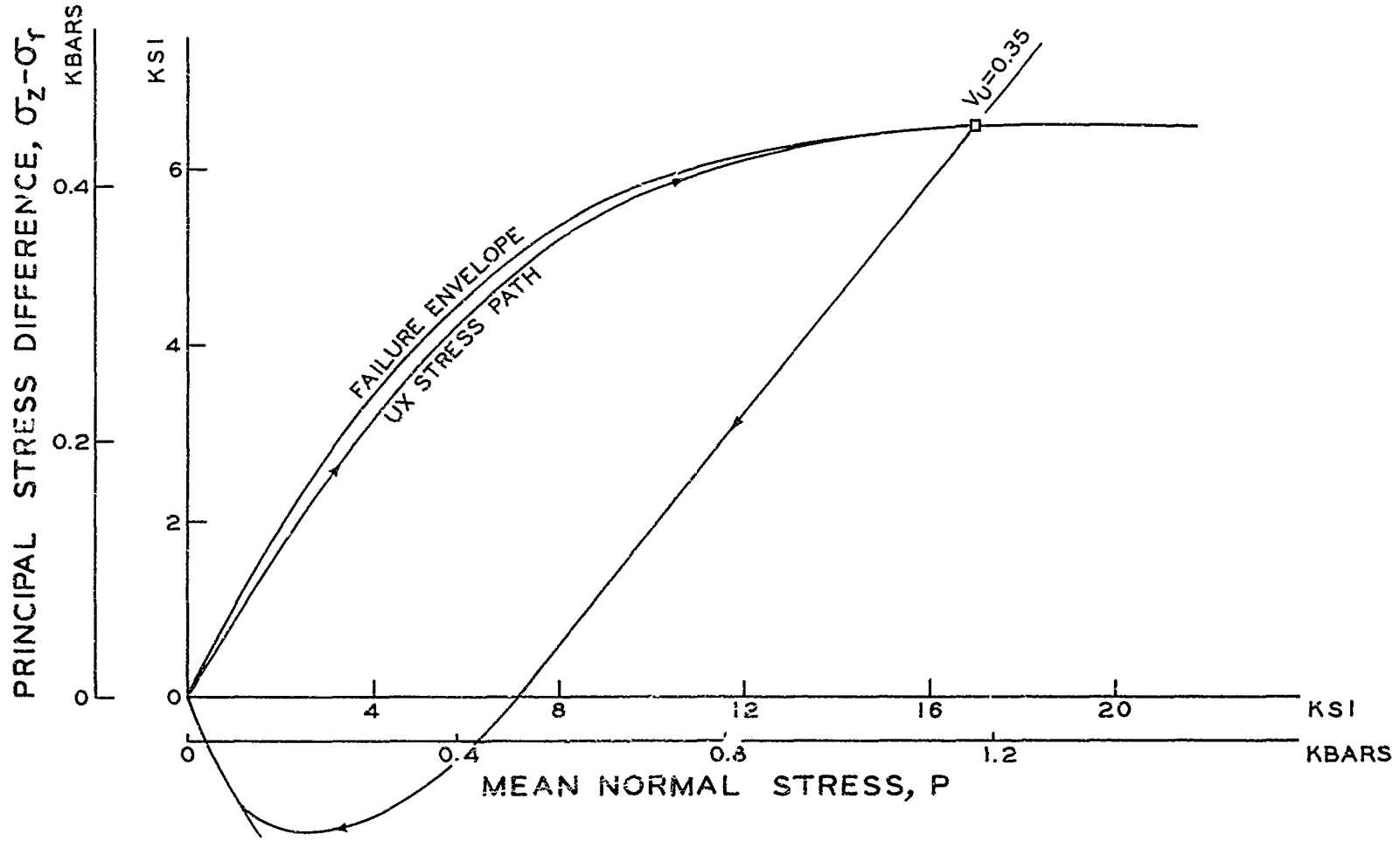

Figure A.10 Representative $(\sigma_z - \sigma_r)$ versus p stress path for uniaxial strain and $(\sigma_z - \sigma_r)_{max}$ versus p failure envelope for triaxial shear to p = 20,000 psi for Layer 1B.

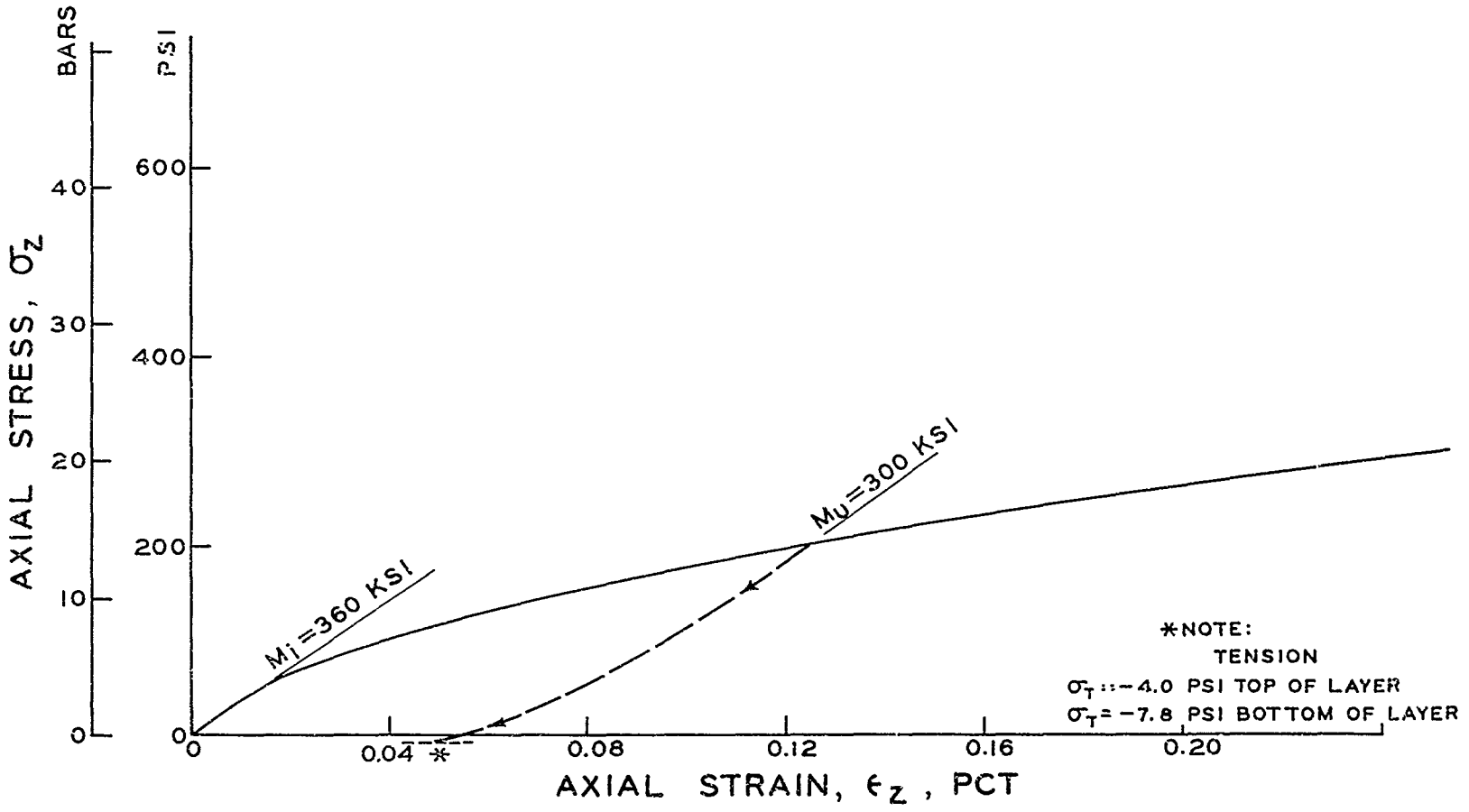

Figure A.11 Representative σ_z versus ε_z relation for uniaxial strain with unloading curve from σ_z = 200 psi for Layer 2.

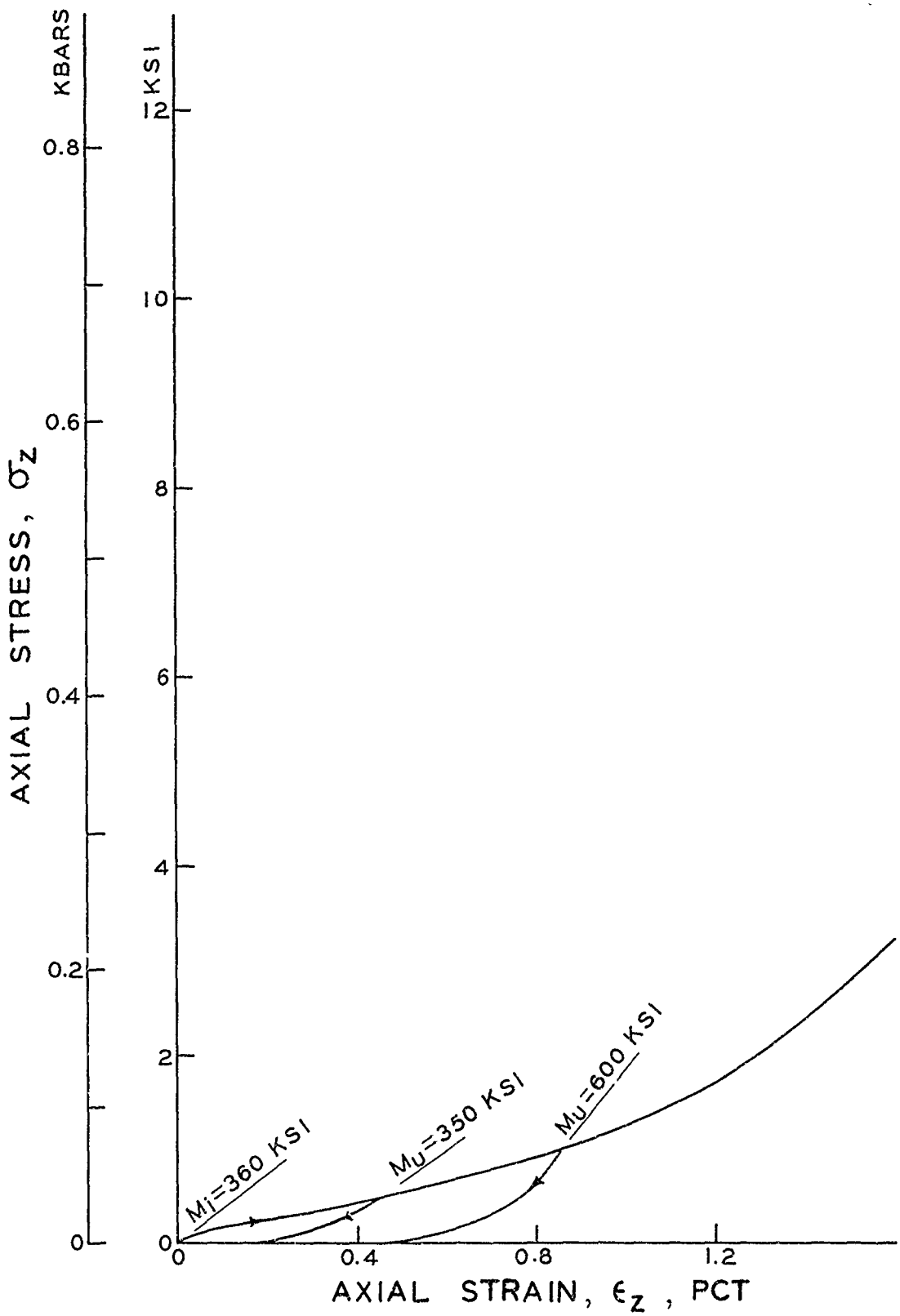

Figure A.12 Representative σ_z versus ε_z relation for uniaxial strain with unloading curves from σ_z = 500 and 1,000 psi for Layer 2.

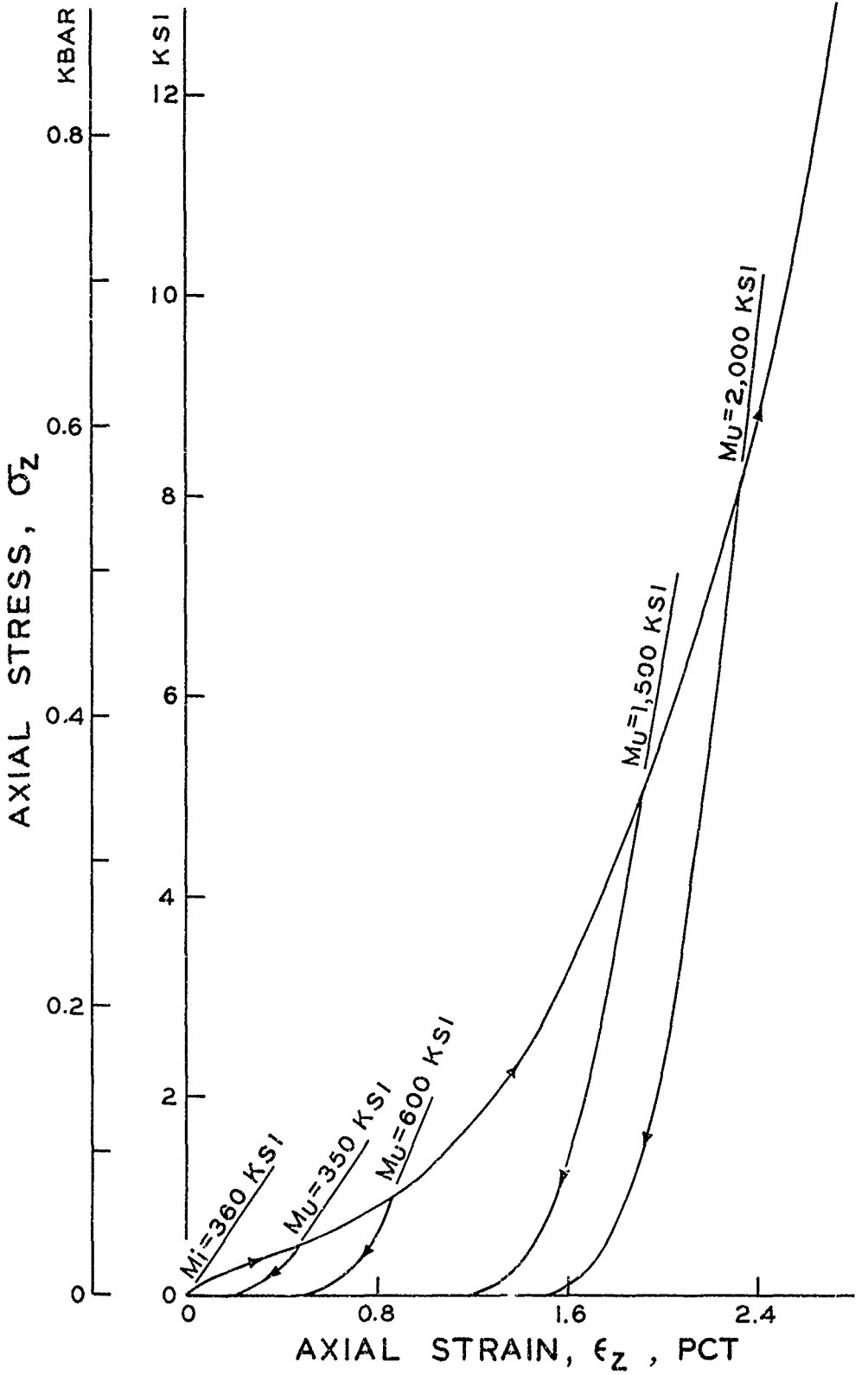

Figure A.13 Representative σ_z versus ε_z relation for uniaxial strain with unloading curves from σ_z = 500, 1,000, 5,000, and 8,000 psi for Layer 2.

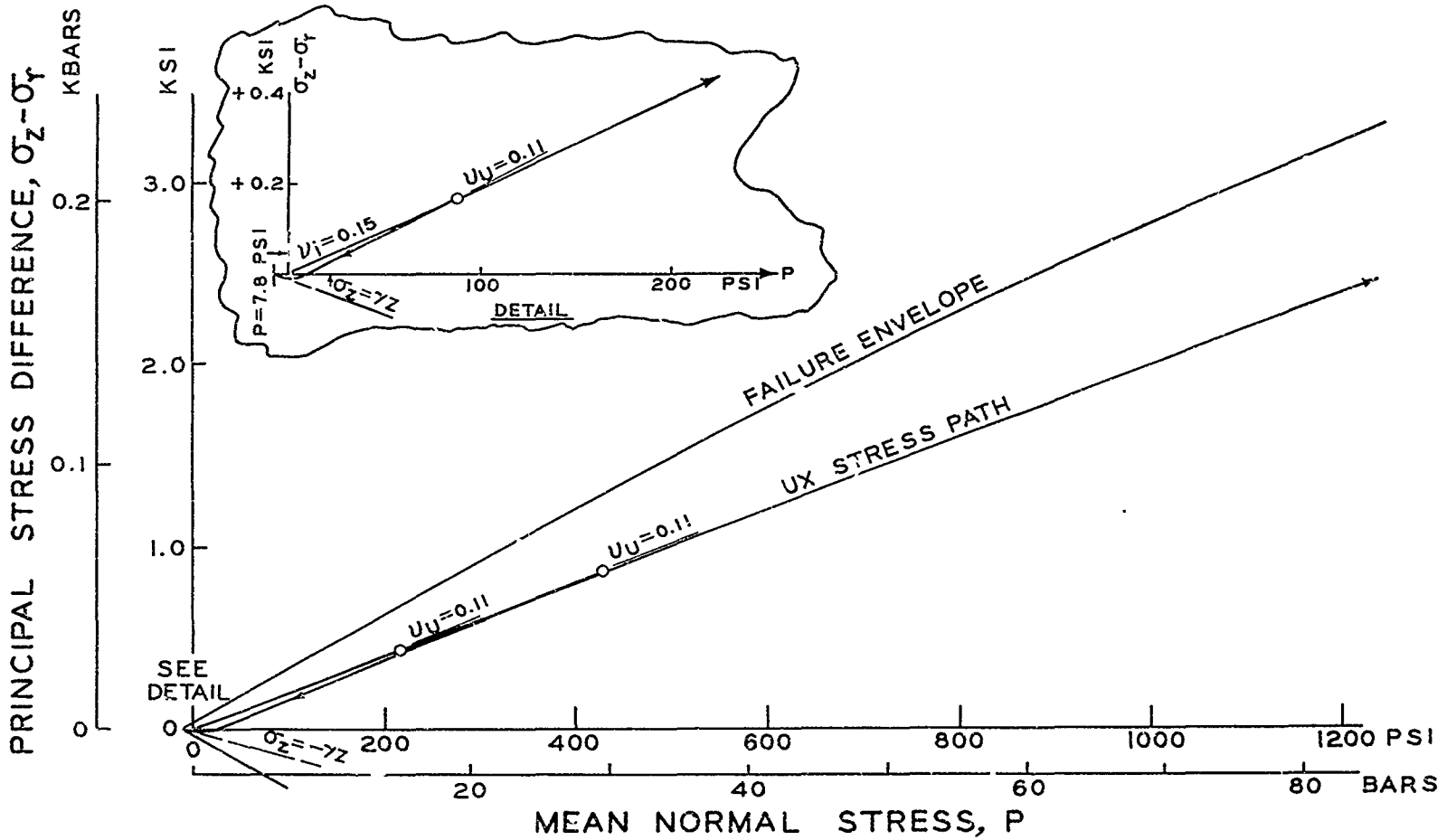

Figure A.14 Representative $(\sigma_z - \sigma_r)$ versus p stress paths for uniaxial strain and $(\sigma_z - \sigma_r)_{max}$ versus p failure envelope for triaxial shear to p = 1,200 psi for Layer 2.

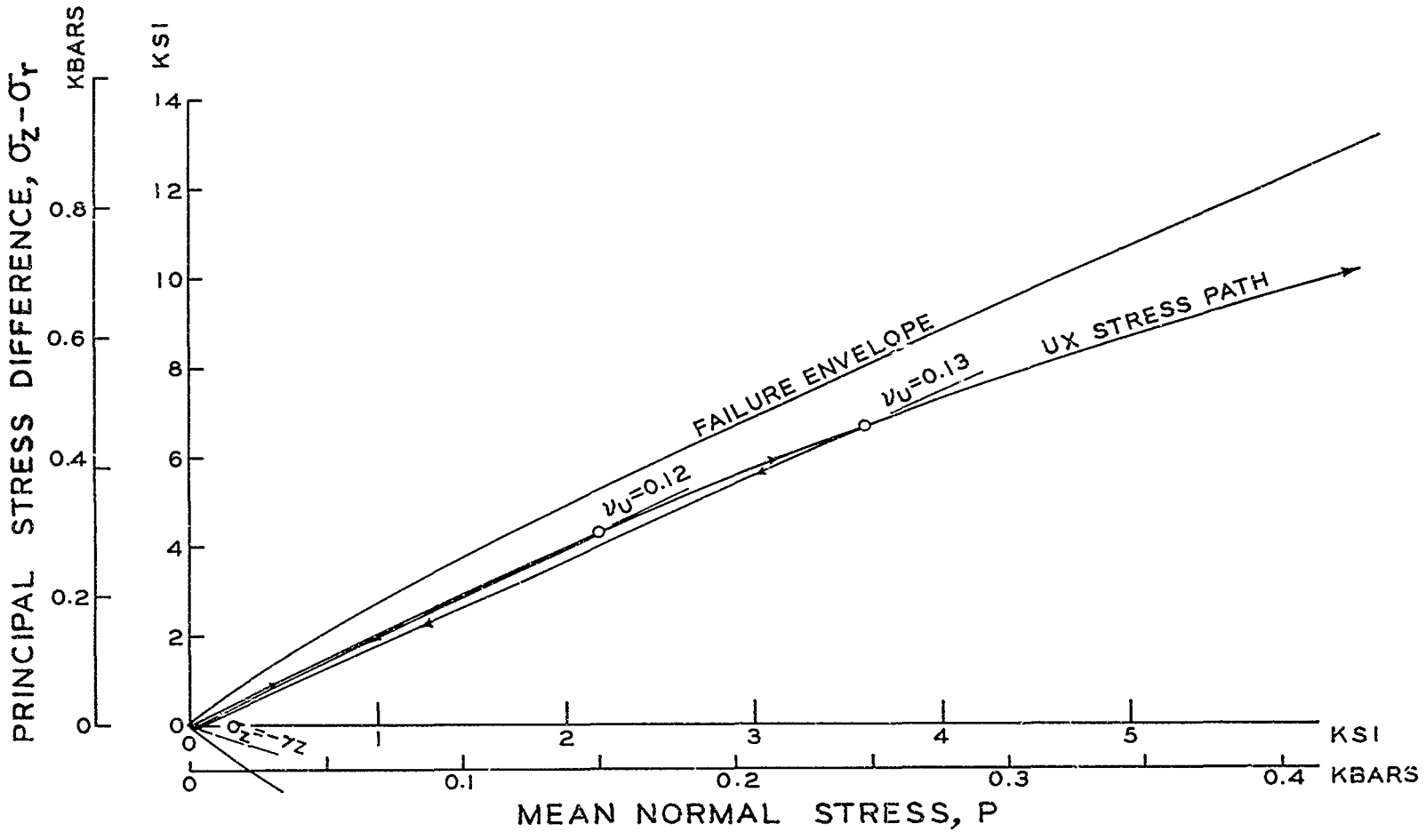

Figure A.15 Representative $(\sigma_z - \sigma_r)$ versus p stress path for uniaxial strain and $(\sigma_z - \sigma_r)_{max}$ versus p failure envelope for triaxial shear to p = 6,000 psi for Layer 2.

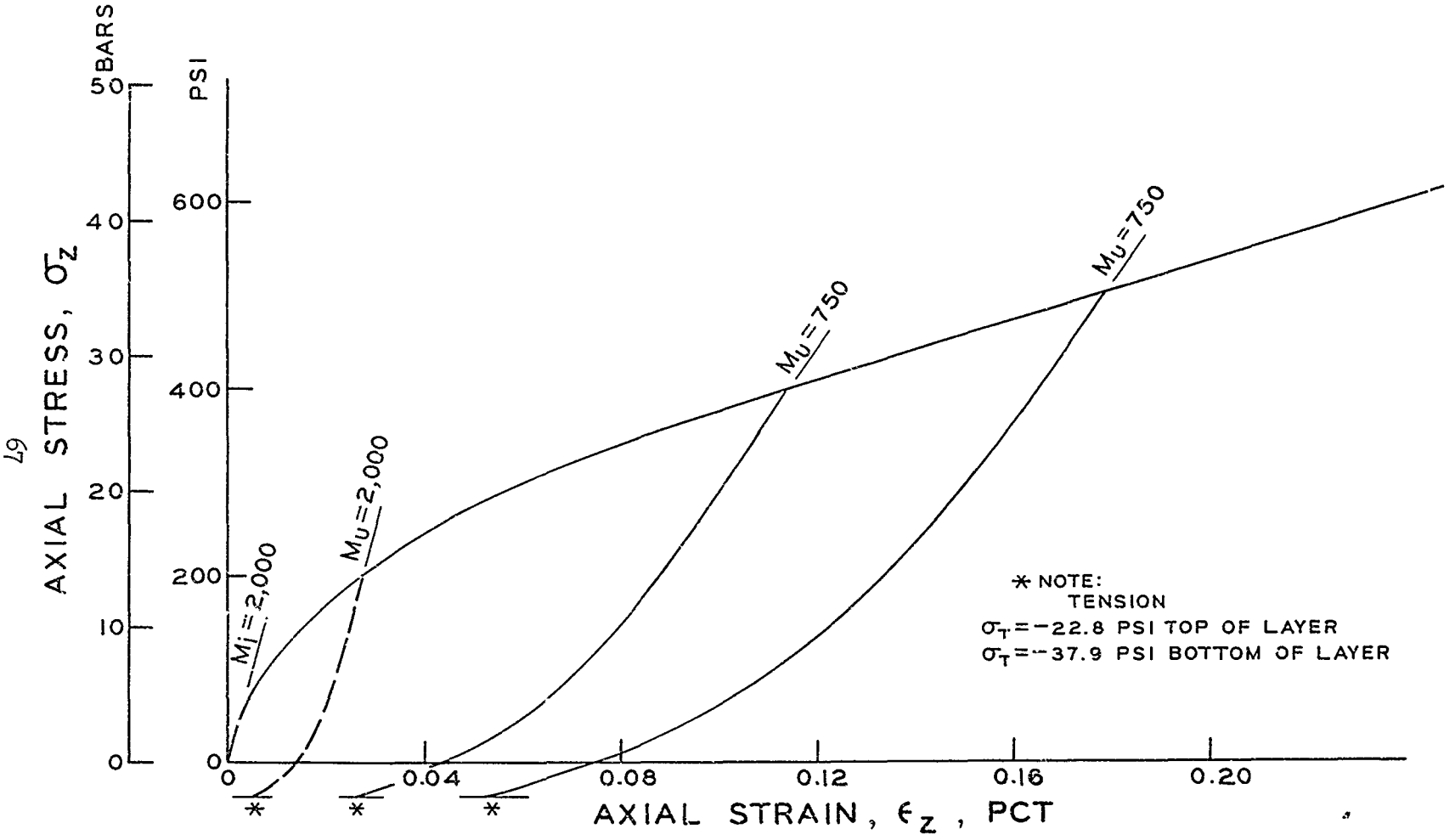

Figure A.16 Representative σ_z versus ε_z relation for uniaxial strain with unloading curves from σ_z = 200, 400, and 500 psi for Layer 3.

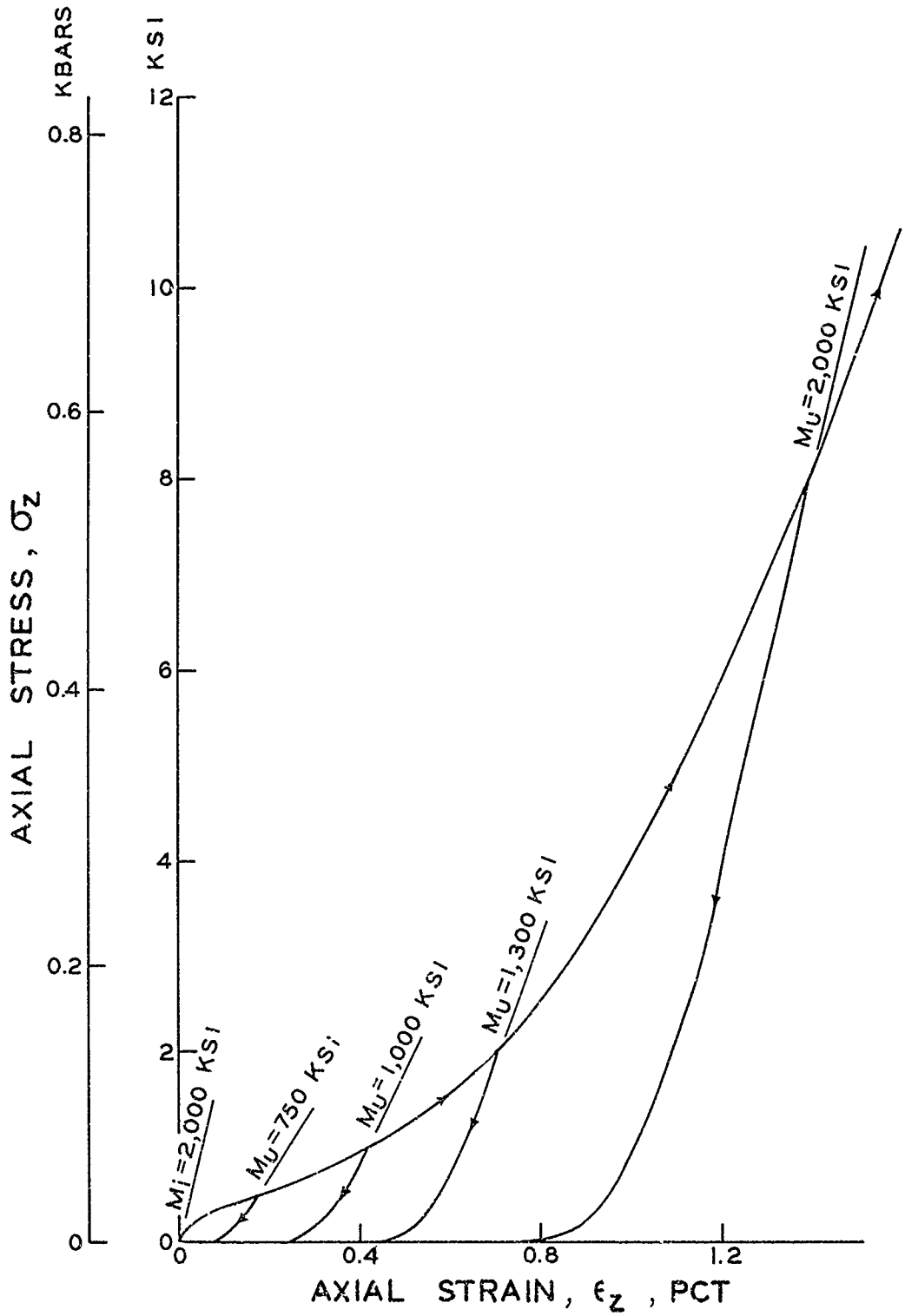

Figure A.17 Representative σ_z versus ε_z relation for uniaxial strain with unloading curves from σ_z = 500, 1,000, 2,000, and 8,000 psi for Layer 3.

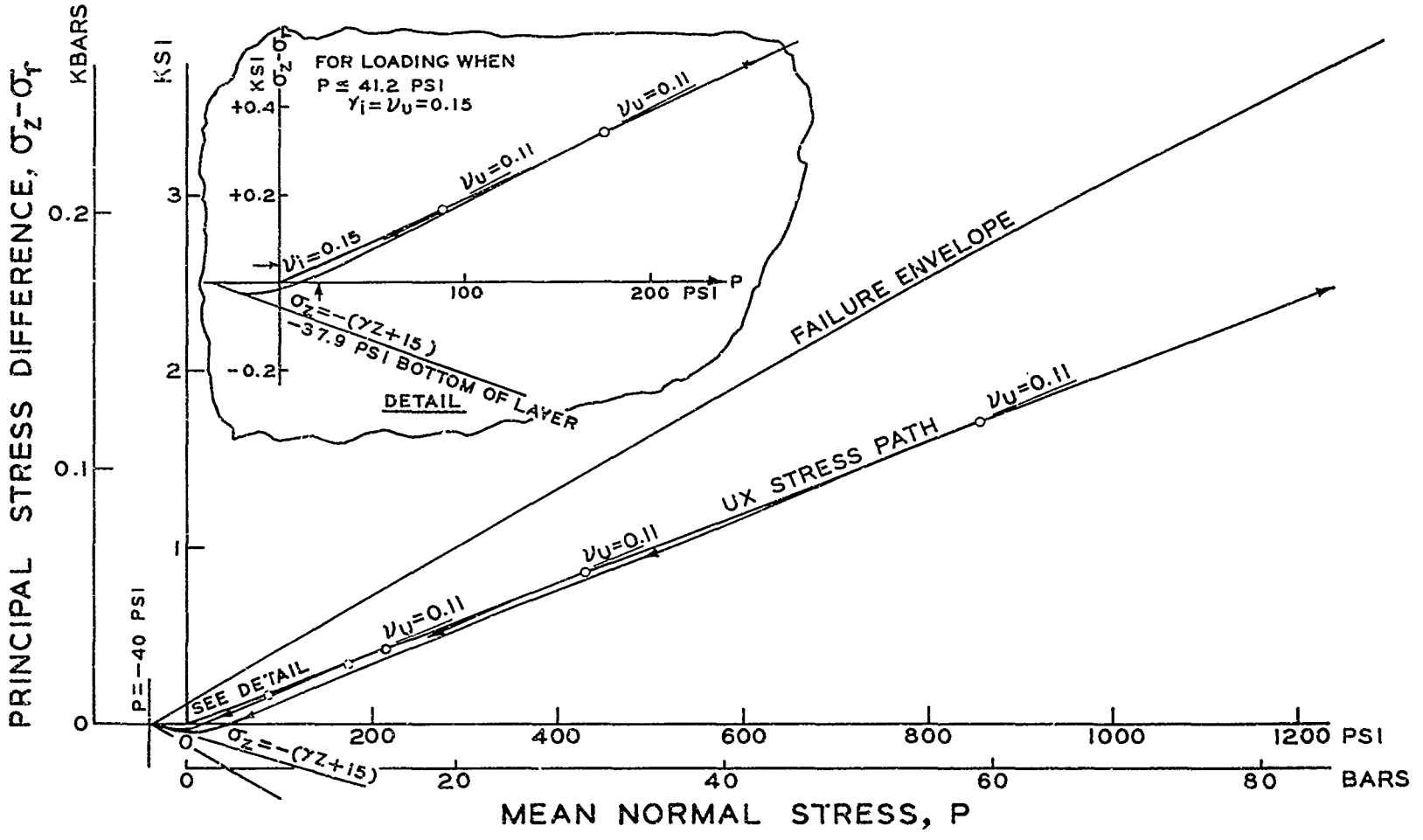

Figure A.18 Representative $(\sigma_z - \sigma_r)$ versus p stress paths for uniaxial strain and $(\sigma_z - \sigma_r)_{max}$ versus p failure envelope for triaxial shear to p = 1,200 psi for Layer 3.

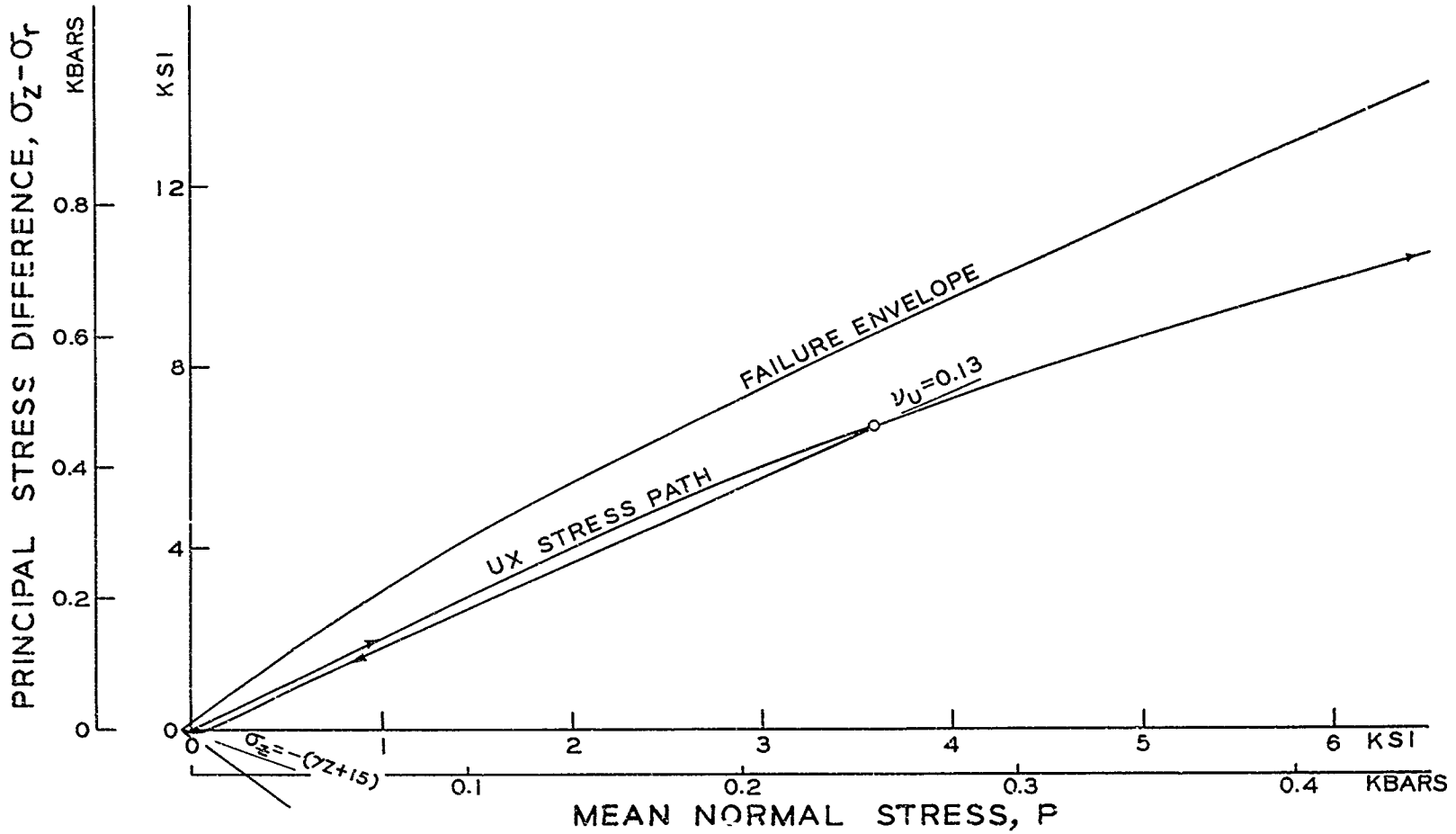

Figure A.19 Representative $(\sigma_z - \sigma_r)$ versus p stress path for uniaxial strain and $(\sigma_z - \sigma_r)_{max}$ versus p failure envelope for triaxial shear to p = 6,000 psi for Layer 3.

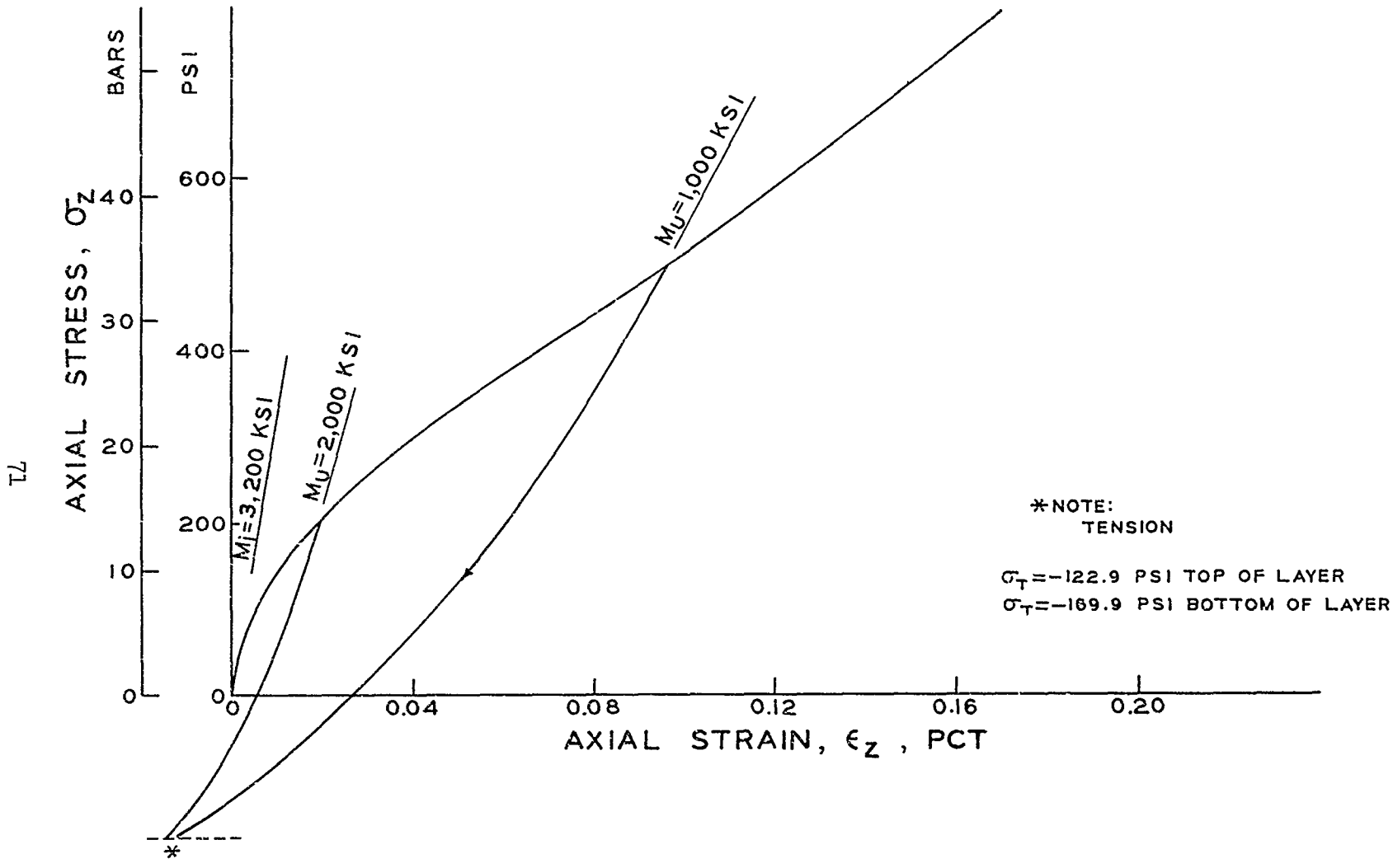

Figure A.20 Representative σ_z versus ϵ_z relation for uniaxial strain with unloading curves from σ_z = 200 and 500 psi for Layer 4.

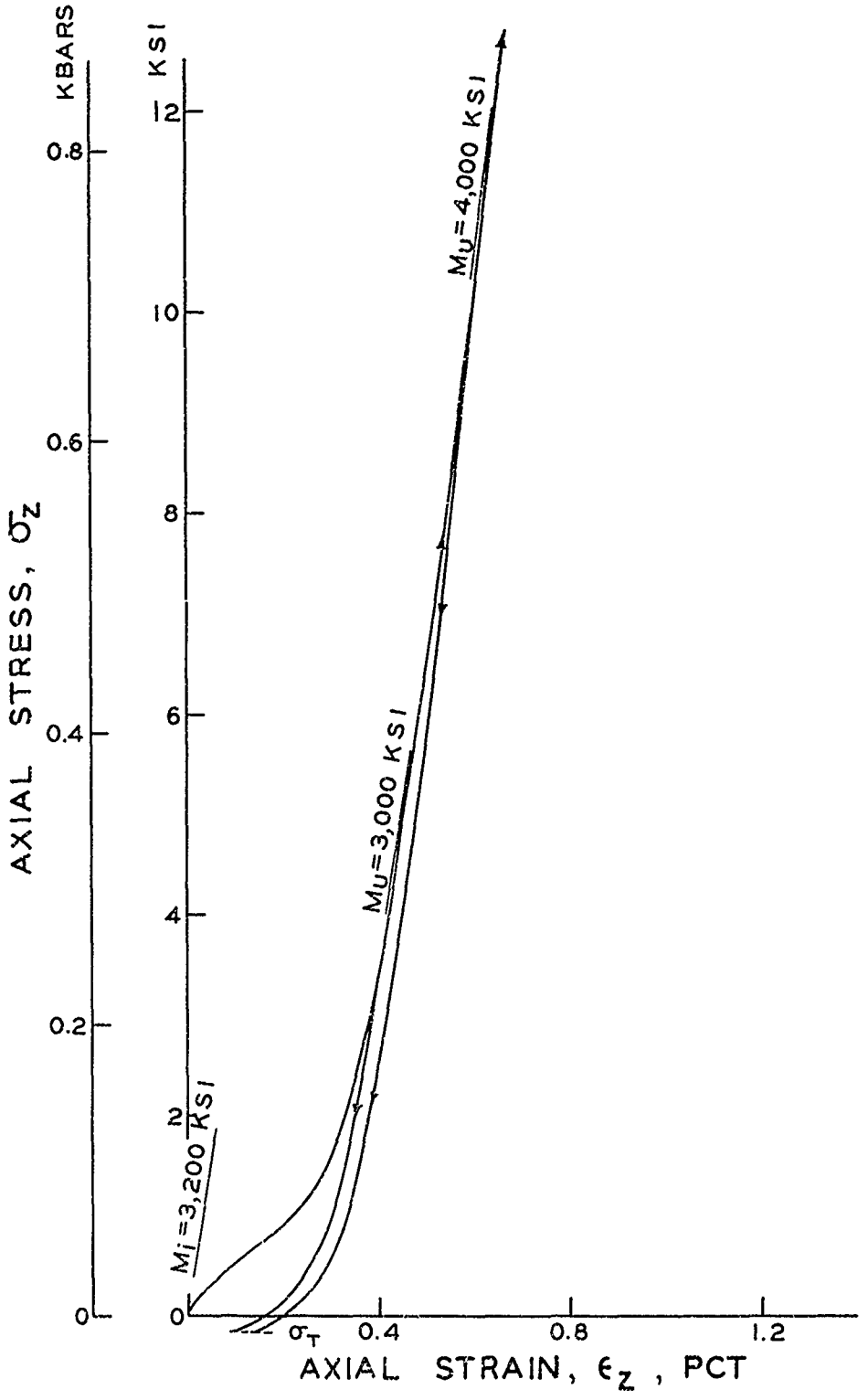

Figure A.21 Representative σ_z versus ε_z relation for uniaxial strain with unloading curves from σ_z = 4,000 and 10,000 psi for Layer 4.

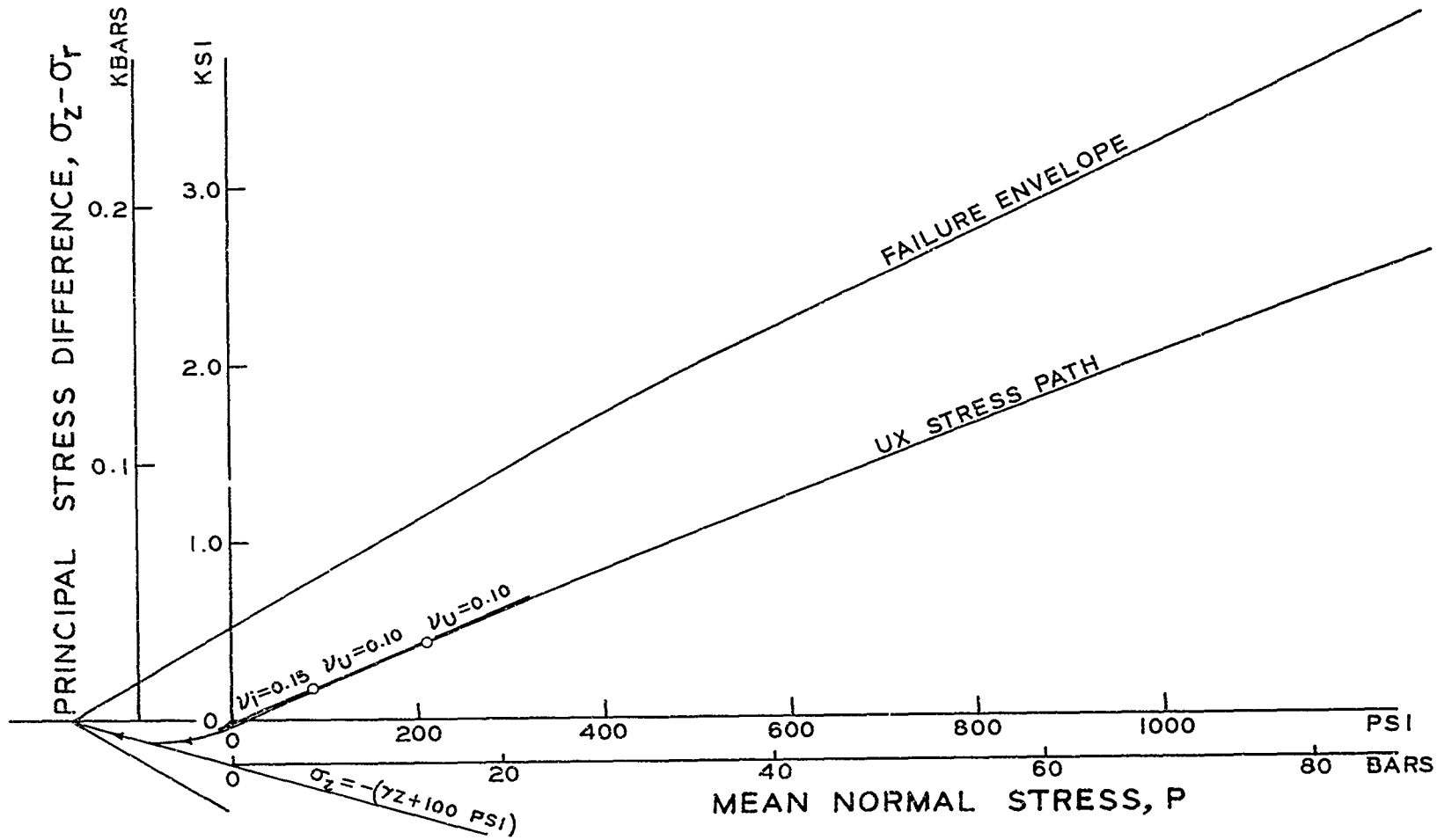

Figure A.22 Representative $(\sigma_z - \sigma_r)$ versus p stress paths for uniaxial strain and $(\sigma_z - \sigma_r)_{max}$ versus p failure envelope for triaxial shear to p = 1,200 psi for Layer 4.

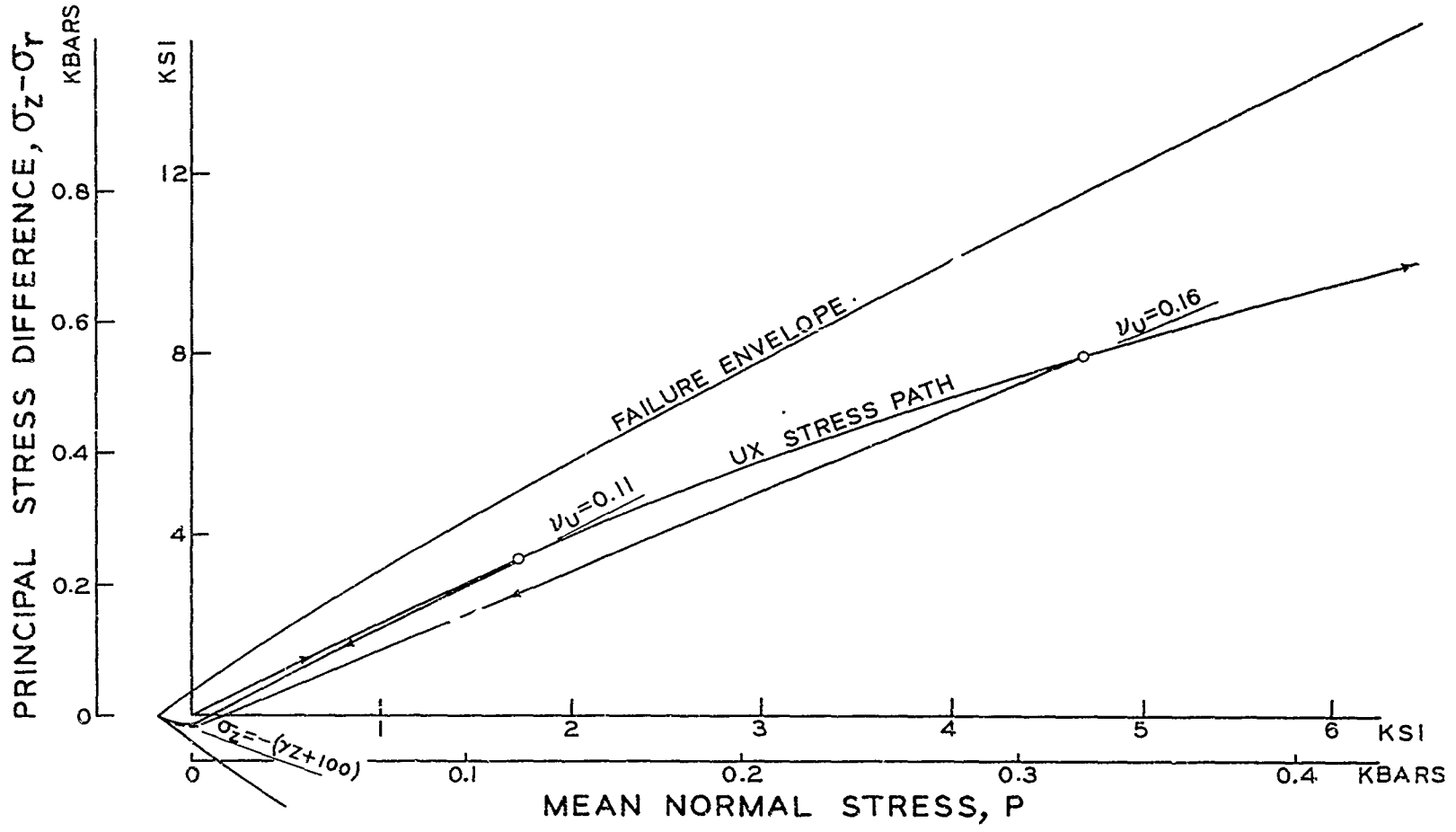

Figure A.23 Representative $(\sigma_z - \sigma_r)$ versus p stress path for uniaxial strain and $(\sigma_z - \sigma_r)_{max}$ versus p failure envelope for triaxial shear to p = 6,000 psi for Layer 4.

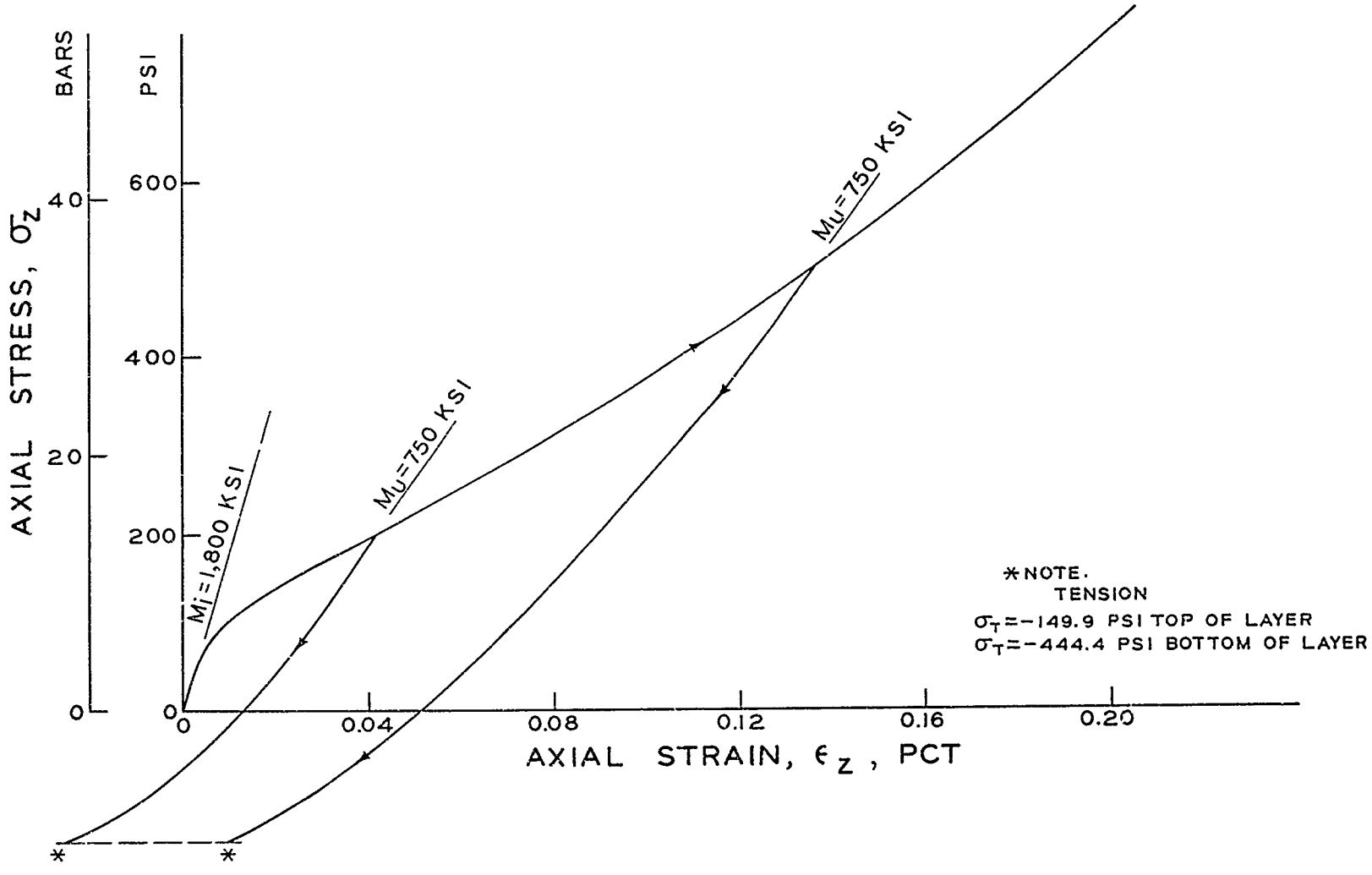

Figure A.24 Representative σ_z versus ε_z relation for uniaxial strain with unloading curves from σ_z = 200 and 500 psi for Layer 5.

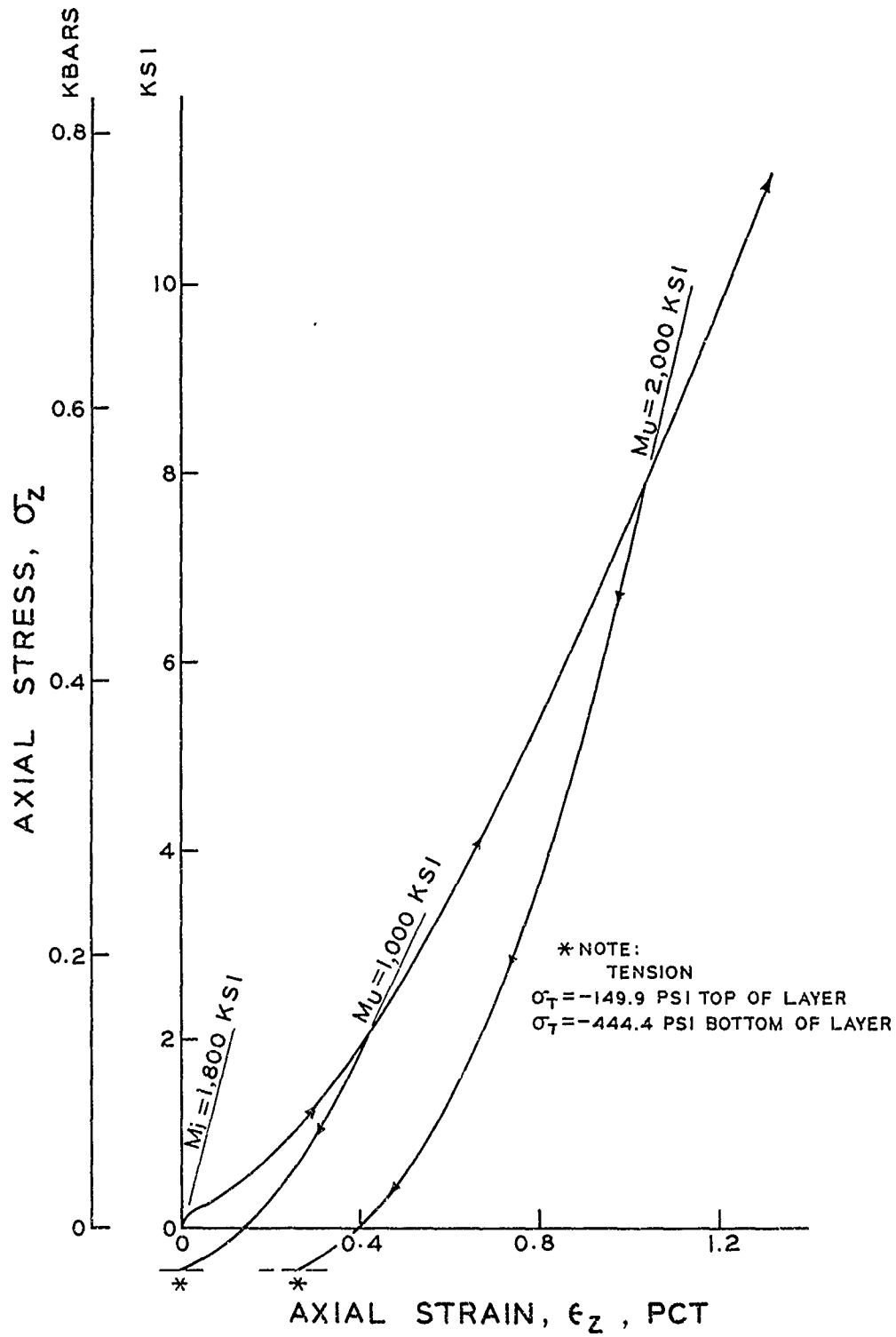

Figure A.25 Representative σ_z versus ϵ_z relation for uniaxial strain with unloading curves from σ_z = 2,000 and 8,000 psi for Layer 5.

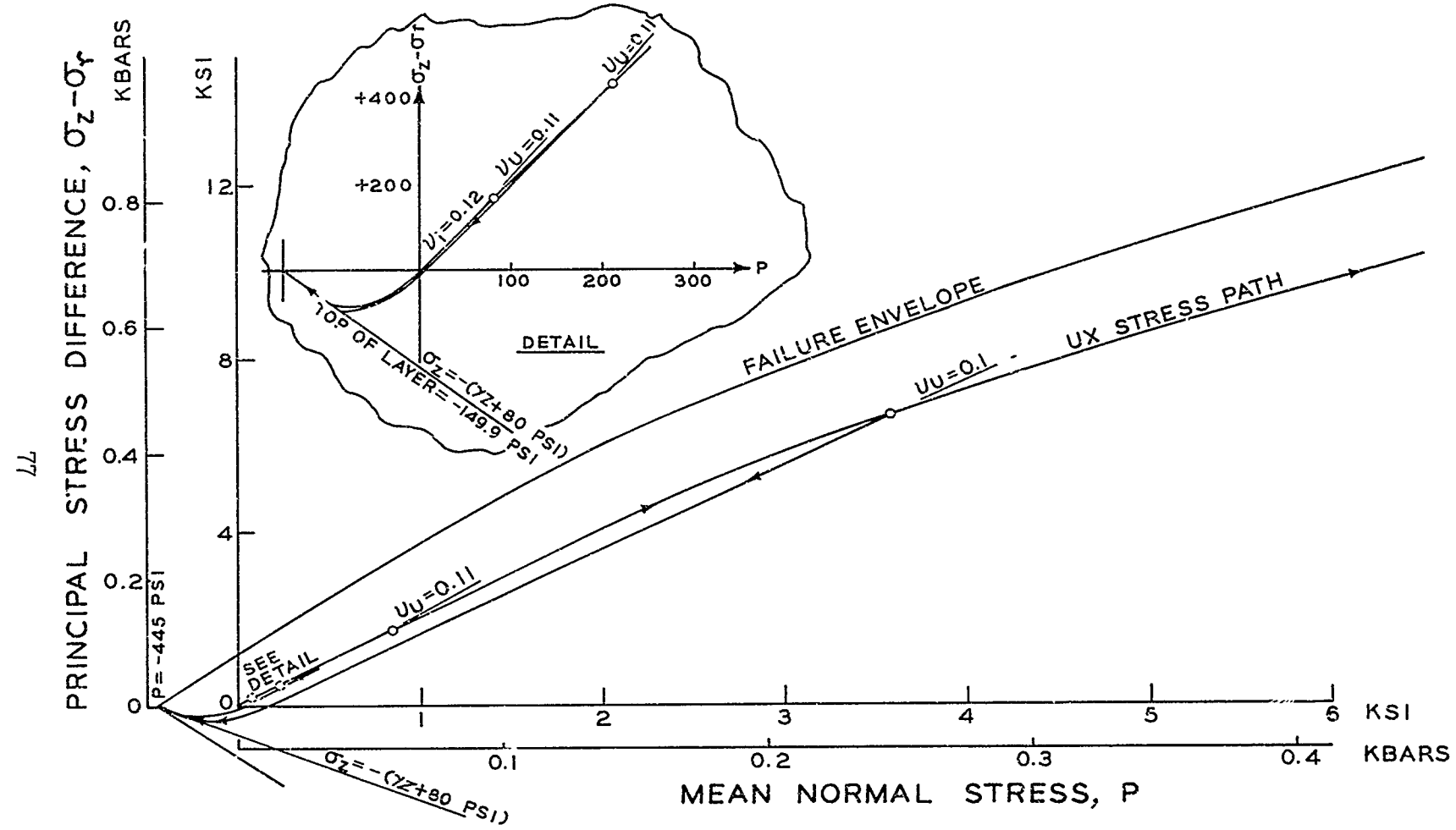

Figure A.26 Representative $(\sigma_z - \sigma_r)$ versus p stress paths for uniaxial strain and $(\sigma_z - \sigma_r)_{max}$ versus p failure envelope for triaxial shear to p = 6,000 psi for Layer 5.

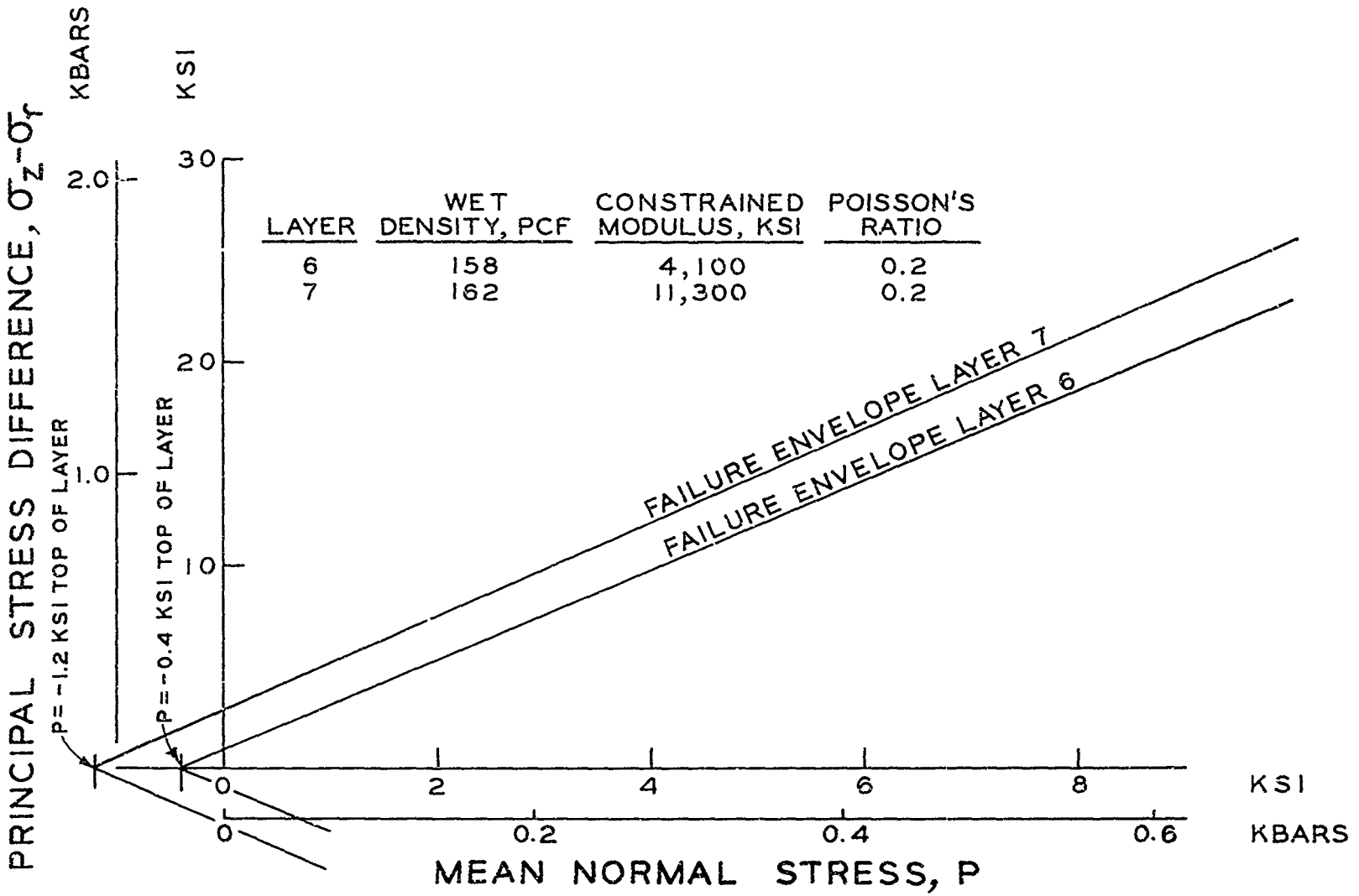

Figure A.27 Table of elastic constants and $(\sigma_z - \sigma_r)_{max}$ versus p failure envelope for triaxial shear to p = 8,000 psi for Layers 6 and 7.